



Published in final edited form as:

J Med Chem. 2010 May 13; 53(9): 3632–3644. doi:10.1021/jm1000612.

Macrocyclic Pyridyl Polyoxazoles: Selective RNA and DNA G-Quadruplex Ligands as Antitumor Agents

Suzanne G. Rzuczek[†], Daniel S. Pilch^{‡,§}, Angela Liu^{‡,§}, Leroy Liu^{‡,§}, Edmond J. LaVoie^{†,§}, and Joseph E. Rice^{*,†}

Department of Medicinal Chemistry, Ernest Mario School of Pharmacy, Rutgers – The State University of New Jersey, 160 Frelinghuysen Road, Piscataway, NJ 08854-8020, USA; Department of Pharmacology, The University of Medicine and Dentistry of New Jersey, Robert Wood Johnson Medical School, Piscataway, NJ 08854-5635, USA; The Cancer Institute of New Jersey, New Brunswick, NJ 08901, USA

Abstract

The synthesis of a series of 24-membered pyridine-containing polyoxazole macrocycles is described. Seventeen new macrocycles were evaluated for cytotoxic activity against RPMI 8402, KB-3, and KB-3 cell lines that overexpress the efflux transporters MDR1 (KBV-1) and BCRP (KBH5.0). Macrocycles in which the pyridyl-polyoxazole moiety is linked by a 1,3-bis(aminomethyl)phenyl group with a 5-(2-aminoethyl)-**18**, or a 5-(2-dimethylaminoethyl)-substituent **19**, displayed the greatest cytotoxic potency. These compounds exhibit exquisite selectivity for stabilizing G-quadruplex DNA with no stabilization of duplex DNA or RNA. Compound **19** stabilizes quadruplex mRNA that encodes the cell-cycle checkpoint protein kinase Aurora A to a greater extent than the quadruplex DNA of a human telomeric sequence. These data may suggest a prominent role for G-quadruplex ligands interacting with mRNA being associated with the biological activity of macrocyclic polyoxazoles. Compound **19** has significant *in vivo* anticancer activity against a human breast cancer xenograft (MDA-MB-435) in athymic nude mice.

Introduction

Compounds that selectively stabilize the G-quadruplex conformation of nucleic acids represent a unique and novel class of anticancer agents.¹ The discovery of the natural product telomestatin, which stabilizes G-quadruplex DNA and inhibits telomerase, prompted research aimed at the design of similar G-quadruplex interactive agents.² Telomestatin (Figure 1), a 24-membered macrocycle comprised of seven oxazole rings and one thiazoline, has a unique molecular architecture that permits efficient π -stacking interactions of its unsaturated heterocyclic rings with p-orbitals on the guanines of a nucleic acid when they are arranged as a planar G-quartet within a quadruplex.³ Studies have suggested that one telomestatin molecule stacks at each terminal G-quartet within a quadruplex to give a 2:1 complex. Moreover, telomestatin stabilizes G-quadruplex DNA in a selective manner, with minimal interaction with duplex DNA.⁴ A large number of polycyclic aromatic hydrocarbons and heterocycles have been designed and synthesized as G-quadruplex stabilizers, but most are less selective than telomestatin.⁵ The design and development of compounds that interact with high selectivity

*To whom correspondence should be addressed. Phone: 732-445-5382. Fax: 732-445-6312. jrice@rci.rutgers.edu.

[†]Department of Medicinal Chemistry

[‡]Department of Pharmacology

[§]The Cancer Institute of New Jersey

with G-quadruplexes are critical to the elucidation of the pharmacological effects of such agents and for establishing the potential clinically utility of this class of anticancer agents.⁶

Recently the synthesis of a series of 24-membered macrocycles incorporating six oxazole rings (two trisoxazole arrays) joined through an amino acid residue has been reported.⁷ The lead compound HXDV (**H**exa**o**xazole-**d**ivaline) has two valine residues connecting the tris-oxazole moieties and stabilizes G-quadruplex DNA to an extraordinary degree with no detectable stabilization of single stranded, duplex, or triplex DNA (Figure 1).^{7c} HXDV has moderate cytotoxicity towards tumor cells (average IC₅₀ ~0.5 μM), which is comparable to that reported for telomestatin.⁸ HXDV induces robust apoptosis in both telomerase positive and telomerase negative cells within 16 h, causes M-phase cell cycle arrest, and reduces the expression of the M-phase checkpoint regulator Aurora A.⁹ These effects are not observed for the non-G-quadruplex stabilizing 24-membered macrocycle TXTLeu (tetraoxazoletetraleucine, Figure 1). Formulation of HXDV for *in vivo* assessment of its antitumor activity proved difficult given its physicochemical properties. Efforts were focused on developing analogs that retain the exquisite selectivity for G-quadruplexes, exhibit enhanced anticancer activity in cell cultures, and possess improved physicochemical properties to permit facile formulation and *in vivo* administration. Towards this goal HXDV analogs with water-solubilizing aminoalkyl groups having two to four-carbon chains replacing one or both isopropyl groups were synthesized and evaluated for their ability to selectively stabilize G-quadruplex DNA and for their cytotoxicity towards tumor cells.¹⁰ Each analog that was prepared in these studies required a lengthy (> 20 step) synthesis that is not readily amenable to the synthesis of quantities of compound that might be required for extensive *in vivo* evaluation against various human tumor xenografts. It was reasoned that a new structure scaffold was needed that can be readily prepared on a multigram scale and easily modified to provide a variety of macrocyclic analogs for evaluating the effect of structure on selective G-quadruplex stabilization and antitumor activity. The design and synthesis of such a scaffold and its elaboration into a series of 24-membered macrocycles is the subject of this investigation. Cytotoxicity data is provided for each targeted macrocycle. On the basis of these data, compound **19** was selected and evaluated for *in vivo* efficacy against the human breast tumor xenograft MDA-MB-435. In addition, the potential of several of these compounds to selectively stabilize G-quadruplexes formed in DNA and RNA was determined.

Results and Discussion

Previous results from our laboratories suggested that a somewhat planar or slightly puckered 24-membered macrocycle with a minimum of five heterocyclic rings is optimal for efficient G-quadruplex stabilization.⁷ A scaffold having a symmetrical array of five contiguous heterocyclic rings bearing identical functionality at each end was envisioned to which a variety of bifunctional linkers could be connected to complete the macrocycle. For ease of synthesis a pyridine having a bis(oxazole) moiety at the 2- and 6-positions appeared to be a logical choice. Readily-available pyridine-2,6-dicarboxylic acid (**1a**) was condensed with oxazole **2**^{10a} to give bis(amide) **3a** in 80% yield (Scheme 1). The TIPS groups were removed with HF-pyridine complex and the resulting diol was treated with DAST to effect cyclodehydration to the bis(oxazoline).¹¹ Dehydrogenation to tetraoxazole **4a** was accomplished with BrCCl₃/DBU.¹² The esters were then hydrolyzed to afford scaffold **5a** in an overall yield of 64%. A second scaffold **5b** was designed to incorporate a 4-bromo substituent on the pyridine which was intended to provide a point of attachment for a variety of functionality at that position on the completed macrocycle. Compound **5b** was prepared in 47% overall yield from 4-bromopyridine-2,6-dicarboxylic acid¹³ (**1b**) by an analogous route as **5a** except that hydrolysis of the ester groups was achieved by treatment with LiBr and DBU to avoid displacement of the bromine from the pyridine ring.¹⁴

The conversion of **5a,b** into 24-membered macrocycles required them to be condensed with a seven atom bifunctional linker. Among the linkers initially employed for this purpose were diethylenetriamine, 1,3-bis(aminomethyl)benzene, and 2,6-bis(aminomethyl)pyridine.¹⁵ A dilute solution (2 mM) of **5a** or **5b** in DMF was treated with EDC, HOBt, and 2,6-lutidine followed by the linker and stirred at room temperature for 2 d (Scheme 2). The yields of macrocycles **6a**, **6b**, and **7** were 30%, 35%, and 22% respectively. Macrolactamization using diethylenetriamine proved more challenging as extensive polymerization occurred using the standard procedure. Stirring **5a** for 3 h with copper (II) triflate prior to treatment with EDC, HOBt, and the diamine linker allowed for macrolactamization to occur to give macrocycle **8** in 15% yield after 2 d. Presumably the copper acts as a template to hold the open ends of **5a** in a conformation more favorable for macrocyclization.

The replacement of one or two oxazole rings by thiazoles was also investigated (Scheme 3). To that end treatment of **3a** with one equivalent of Lawesson's reagent¹⁶ in toluene at 80 °C gave monothioamide **9a** in good yield. In the presence of excess Lawesson's reagent bis (thioamide) **9b** was formed. The conversion of **9a,b** into pyridyl tetraazole derivatives **10a,b** in overall yields of 56% and 79% respectively was achieved using an identical sequence as employed for **4a,b**. The esters were hydrolyzed with LiOH and macrocyclization of **10a** with 1,3-bis(aminomethyl)benzene afforded **11a** in 33% yield. Surprisingly, similar treatment of **10b** failed to give any of the bis(thiazole) macrocycle **11b**. Performing the macrocyclization in a step-wise manner however, provided a solution to this problem. Thus condensation of **10b** with the commercially-available mono-Boc derivative of 1,3-bis(aminomethyl)benzene followed by treatment with TFA afford the monoamide in 68% for the two steps. Macrocyclization using EDC then gave the desired macrocycle **11b** in 43% yield.

The ability to prepare macrocycles having water-solubilizing groups attached to either the pyridine or phenyl ring was a critical element to allow for the test compounds to be readily formulated and administered in the assessment of their *in vivo* antitumor activity. It was envisioned that a suitably positioned halide on either the pyridine ring, as in **6b**, or on the phenyl ring could serve as a handle for the attachment of substituents *via* transition-metal catalyzed coupling reactions. To that end 1,3-bis(aminomethyl)-5-bromobenzene **12** was prepared¹⁷ as an additional linker (Scheme 4). Macrocyclization of **12** with **5a** and **5b** afforded compounds **13a** and **13b** in 58 and 22% yield, respectively. Unfortunately, all attempts to derivatize **6b**, **13a**, or **13b** by Suzuki-Miyaura coupling with potassium [2-(benzyloxycarbonylamino)ethyl]trifluoroborate¹⁸ led primarily to the de-bromo compound **6a**. It is possible that the intact macrocycle chelates the palladium catalyst and prevents it from participating in the coupling reaction.

The water-solubilizing substituent could, however, be attached to the phenyl linker prior to macrocyclization. This required that the primary amino groups of **12** be protected as *tert*-butyl carbamate (Boc) derivatives (Scheme 5). Suzuki-Miyaura coupling of the resulting bromo compound with the same trifluoroborate reagent in the presence of PdCl₂(dppf).CH₂Cl₂ and Cs₂CO₃ afforded the desired product **14a** in 79% yield. Removal of the Boc groups with trifluoroacetic acid (TFA) and macrocyclization with **5a** and **5b** afforded compounds **15a** and **15b** in identical 42% yields. Removal of the Cbz group from **15a**, however, proved troublesome under a variety of hydrogenolysis conditions, affording the primary amine in very low yield. Therefore **14a** was subjected to hydrogenolysis over Pd(OH)₂/C to remove the Cbz group in quantitative yield. Protection of the amine as a trifluoroacetamide (TFAA, pyridine) was then followed by removal of the Boc groups (TFA) gave diamine **16**. Macrocyclization of **16** with **5a** afforded compound **17** in 25% yield. The trifluoroacetamide was removed upon treatment with K₂CO₃ in MeOH to give **18**. A portion of **18** was reductively methylated using aqueous formaldehyde and sodium triacetoxyborohydride to give the N,N-dimethylamino derivative **19**.

The synthesis of a third scaffold having a basic side-chain attached to the pyridine ring (Scheme 6) proved necessary due to our inability to derivatize bromo compound **6b**. Chelidonic acid (4-hydroxypyridine-2,6-dicarboxylic acid) was coupled with oxazole **2** to form bis(amide) **20**. Treatment with N-(3-bromopropyl)phthalimide and DBU afforded pyridyl ether **21**. Removal of the TIPS protecting groups, cyclodehydration with DAST, and dehydrogenation with BrCCl₃/DBU gave scaffold **22** after removal of the ester groups using LiCl in refluxing DMF. This was subjected to macrocyclization using 1,3-bis(aminomethyl)benzene, **12**, and **14a** (after removal of the Boc groups) to give macrolactams **23a-c**. Treatment of **23a** with hydrazine hydrate gave primary amine **23d**.

Each macrocycle was evaluated for cytotoxic activity against human lymphoblastoma RPMI 8402, human epidermoid carcinoma KB3-1, and KB3-1 cell lines that overexpress the efflux transporters MDR1 (KBV-1) and BCRP (KBH5.0) (Table 1). The parent macrocycle **6a**, with a 1,3-bis(aminomethyl)phenyl group linking the ends of scaffold **5a** displays modest cytotoxic potency against RPMI 8402 and KB3-1 (IC₅₀ ~1 μM). Replacement of that linker with either 2,6-bis(aminomethyl)pyridyl, **7a**, or diethylenetriamine, **8**, results in a loss of activity. The replacement of one oxazole ring of **6a** with a thiazole (**11a**) resulted in a four-fold increase in activity against KB3-1, but had no effect on RPMI 8402 cells. Substitution of a second oxazole by thiazole (**11b**), however, resulted in a complete loss of activity. The loss of activity for diethylenetriamine derivative **8** might be related to its less rigid structure as compared to **6a**, although the effect of including a strongly basic secondary amine within the macrocycle cannot be discounted. A substantial difference in lipophilicity exists between thiazole (log P = 0.77) and oxazole (log P = -0.59), which may help to explain why substitution of a second oxazole by thiazole (compound **11b**), results in a loss of activity relative to monothiazole **11a**. At the present time, however, we can offer no explanation for the results obtained with dipyrindyl derivative **7a**.

Attachment of a single bromine at either the 5-position of the benzene ring (**13a**) or the 4-position of the pyridine **6b** results in a three-fold increase in cytotoxic potency against RPMI 8402 and about a 10-fold increase in activity against KB3-1 as compared to unsubstituted benzene derivative **6a**. Simultaneous substitution of bromine on both the benzene and pyridine rings (**13b**), however, results in a loss of all activity. This might again be an effect of the increased lipophilicity of **13b** as opposed to **6b** and **13a**. A similar, although not so dramatic, trend is observed for the 5-[2-(benzyloxycarbonylamino)ethyl]-1,3-bis(aminomethyl)phenyl-linked macrocycles **15a** and **15b**. Compound **15a** which is unsubstituted on the pyridine is five to ten times more active than **15b** which has a bromine on the 4-position of the pyridine ring. The Cbz-protected 2-aminoethyl derivative **15a** is approximately one order of magnitude more potent than parent compound **6a**. A change in the amine protecting group to trifluoroacetamide **17** has little effect on activity. Both primary amine **18** and tertiary amine **19** have potent activity (30–40 nM) against KB3-1 cells and slightly weaker activity (90–180 nM) against RPMI 8402 cells. It is also noteworthy that while **18** and **19** are both substrates for MDR1, as evidenced by their total lack of activity against KBV-1. They retain similar cytotoxicity against KBH5.0 relative to KB3-1 cells indicating that they are not substrates for the efflux transporter BCRP.

The effect of attachment of a large group (OCH₂CH₂CH₂NPhth) on the pyridine ring at its 4-position was to substantially lower activity. For example comparison of 4-bromophenyl derivatives **23b** and **13a** reveals a 3–16 fold loss of activity for the substituted pyridyl derivative **23b** in RPMI 8402 and KB3-1 cells. Similarly for compounds having a protected 2-aminoethyl substituent on the phenyl ring, activity drops from 120 nM for **15a** to >10 μM with the attachment of the large substituent on the pyridine ring (**23c**). Within this series only **23a** with an unsubstituted phenyl ring exhibited moderate activity against KB3-1 cells (0.4 μM), but was largely inactive (IC₅₀ 4.5 μM) against the RPMI 8402 cell line. Changing the nature of

the terminal group on the (3-aminopropyl)oxy to primary amine **23d** did not enhance cytotoxic potency.

HXDV and four selected macrocyclic pyridyl polyoxazoles (**6a**, **11b**, **18**, and **19**) were evaluated for their ability to selectively bind and stabilize quadruplex versus duplex DNA and RNA in the presence of physiological concentrations of K^+ ions (150 mM). We used salmon testes (ST) DNA and poly(rA)•poly(rU) as representative models of duplex DNA and RNA, respectively. As a representative model of quadruplex DNA, we used the human telomeric sequence d[T₂G₃(T₂AG₃)₃A], which we denote as hTel. Patel and coworkers have shown that the structure adopted by d[T₂G₃(T₂AG₃)₃A] in K^+ solution is an intramolecular (3 + 1) G-quadruplex in which three strands are oriented in one direction and the fourth strand is oriented in the opposite direction.¹⁹ In an effort to explore ligand binding interactions with quadruplex RNA, we used a putative quadruplex-forming sequence (r[AG₄CG₂CUG₂UCG₂AGUG₂C]) derived from the 5'-untranslated region of the mRNA that encodes the cell-cycle checkpoint protein kinase Aurora A (AurA).

Figure 2 shows the UV melting profiles (depicted in their first derivative forms) of the four nucleic acids described above in the absence and presence of HXDV and **19**. The ligand-induced changes, if any, in the transition temperatures (T_{tran}) corresponding to the maxima or minima of these first-derivative melting profiles are listed in Table 2, as are the corresponding changes in T_{tran} values derived from melting profiles (not shown) conducted in the presence of **6a**, **11b**, and **18**. The presence of neither ligand alters the thermal stability of ST duplex DNA or poly(rA)•poly(rU) duplex RNA to any significant extent, with any observed changes in T_{tran} being within the experimental uncertainty. This observation is consistent with little or no duplex DNA or RNA binding on the part of any of the five macrocyclic polyoxazoles tested here. We previously observed a similar behavior for HXDV.^{7,10}

In marked contrast to their negligible impacts on the thermal stabilities of the DNA and RNA target duplexes, HXDV, **6a**, **18**, and **19** increase the T_{tran} value of the hTel DNA quadruplex by 11.5, 7.5, 21.0, and 20.5 °C, respectively. These results are not only indicative of binding to hTel, but also provide information with regard to the relative affinities of the compounds for the host DNA quadruplex. In this connection, the relative extents to which ligands stabilize a target nucleic acid are typically correlated with the relative binding affinities of the ligands for the target.²⁰ Our hTel UV melting results are therefore consistent with the affinities of HXDV, **6a**, **18**, and **19** for the target DNA quadruplex following the hierarchy **18** ≈ **19** > HXDV > **6a**. It is perhaps not surprising that **18** and **19** exhibit a greater apparent affinity for the hTel quadruplex than HXDV or **6a**, since, unlike HXDV and **6a** (which are nonionic), **18** and **19** both contain basic amine functionalities that adopt positive charges at the physiologically relevant pH of 7.5 used in the UV melting studies. Note that, unlike HXDV, **6a**, **18**, and **19**, compound **11b** exerts no impact on the thermal stability of the hTel quadruplex. This observation coupled with the duplex results described above suggests that **11b** binds neither the duplex nor the quadruplex nucleic acid form. The lack of quadruplex binding by **11b** may be a consequence of the two thiazole moieties in this compound.

The temperature-induced hypochromic transition at 295 nm exhibited by the AurA RNA sequence in the absence of ligand (see Figure 2D) indicates that this RNA oligomer does indeed adopt a quadruplex structure in the presence of 150 mM K^+ . Moreover, the presence of HXDV and **19** enhance the thermal stability of AurA RNA quadruplex by 19.5 and 37.0 °C, respectively. These ΔT_{tran} values are significantly greater than the corresponding values (11.5 °C for HXDV and 20.5 °C for **19**) associated with the binding of these compounds to the hTel DNA quadruplex. Thus, HXDV and **19** appear to target the AurA RNA quadruplex with an even greater affinity than the hTel DNA quadruplex. Our collective UV melting studies indicate

that macrocyclic polyoxazoles bind the quadruplex nucleic acid form with a high degree of specificity, with their affinities being greater for RNA relative to DNA target quadruplexes.

It is of interest to compare the relative extents to which HXDV, **6a**, **11b**, **18**, and **19** bind and stabilize the quadruplex nucleic acid form with their relative cytotoxic potencies. Toward this end, a comparison of the ΔT_{tran} data in Table 2 with the corresponding cytotoxicity (IC_{50}) data in Table 1 reveals a good correlation between cytotoxic potency and quadruplex stabilizing activity.

Compounds that stabilize G-quadruplex conformations of nucleic acids are viewed as a potential novel class of anticancer agents. Many such compounds have been reported, along with their ability to stabilize G-quadruplex DNA in the test tube.⁵ Cytotoxicity data has also been reported for several of these G-quadruplex stabilizers.^{5d,f} Such *in vitro* studies however, provide little insight into the ability of G-quadruplex stabilizers to penetrate into cancer cells and to stop the growth and destroy cancer cells *in vivo*. Telomestatin is one of the few compounds known to stabilize G-quadruplex DNA for which *in vivo* anticancer activity in a human tumor xenograft has been reported. The results showed that telomestatin does indeed kill such tumor cells in a mouse model.²¹ In comparison with telomestatin however, the compounds reported in the present study are more selective for stabilizing G-quadruplex DNA. The decision was made to synthesize the 2-(N,N-dimethylamino)ethyl substituted analog **19** on a larger scale and to evaluate its antitumor activity *in vivo* against a human breast cancer xenograft (MDA-MB-435) in athymic nude mice. The results from the *in vivo* bioassay of **19** are presented in Figure 3. An experimental group of seven tumor-bearing mice was initially treated with **19** on day 10 and subsequently treated three times a week on alternate days for three weeks at dosing that escalated each week and averaged 32 mg/kg. Despite increasing the dosing from 25 mg/kg to 42 mg/kg, no significant change in body weight was observed during the three weeks of treatment, Table 3. The negative control group, which was treated with only citrate buffer, had an average tumor volume >1350 mm³ after 35 days. In contrast, the tumor-bearing mice treated with **19** had an average tumor volume of <400 mm³ and had a % T/C value of 27.7%. The positive control group was treated three times a week with irinotecan starting on day 0 at a dose of 20 mg/kg and 35 days after initial treatment had an average tumor volume of <100 mm³. These results clearly demonstrate the *in vivo* efficacy of compound **19**.

Conclusions

The results presented above describe an efficient synthesis of pyridyl tetraoxazole platforms that can be performed on a multi-gram scale. A key feature of these syntheses is the symmetry of the central pyridine which allows for the use of only a single oxazole building block to rapidly arrive at a difunctional molecule that is elaborated into a macrocycle in only one step. A wide variety of functionalized diamine linkers can be employed for the macrolactamization. Functionality can also be incorporated on the pyridine ring of the scaffold to allow for the rapid preparation of series of analogs. Of the 17 new macrocycles reported herein those employing a 1,3-bis(aminomethyl)phenyl linker with a 5-(2-aminoethyl) **18** or a 5-(2-dimethylaminoethyl) substituent **19** displayed the greater cytotoxic potency. These compounds exhibited exquisite selectivity for stabilizing G-quadruplex DNA with no stabilization of duplex DNA or RNA. Compound **19** stabilizes quadruplex mRNA that encodes the cell-cycle checkpoint protein kinase Aurora A to an even greater extent than quadruplex DNA. These data may suggest a prominent role for G-quadruplex ligands interacting with mRNA being associated with the biological activity of macrocyclic polyoxazoles. The anticancer activity of **19** was evaluated *in vivo* against a human breast cancer xenograft (MDA-MB-435) in athymic nude mice. Results from this bioassay indicate that **19** has significant *in vivo* efficacy as an anticancer agent and administration of doses of **19** increasing from 25 mg/kg to 42 mg/kg did not result in weight loss or other observable adverse effects in mice. The synthetic methodology

outlined will permit more in depth studies on the structure-activity relationships associated with the stabilization of various types of G-quadruplexes. The increased accessibility of test compounds within this series of G-quadruplex stabilizers relative to macrocyclic hexaoxazoles will also allow for expanded studies on the pharmacological properties of these highly selective G-quadruplex stabilizers.

Experimental Section

Chemistry

All reactions were conducted under an atmosphere of argon in oven-dried glassware unless otherwise noted. THF was dried by distillation from sodium-benzophenone. Toluene, CH_2Cl_2 , 2,6-lutidine, Et_3N , pyridine, DBU, and CH_3CN were freshly distilled from CaH_2 . Anhydrous DMF was obtained by stirring overnight over anhydrous CuSO_4 followed by distillation under reduced pressure. All starting materials and reagents were commercially available and were used as received with the exception of 4-bromopyridine-2,6-dicarboxylic acid¹³ (**1b**), 1-bromo-3,5-bis(aminomethyl)benzene¹⁷ (**12**) and 2,6-bis(aminomethyl)pyridine¹⁵ which were prepared as described previously. Flash chromatography was conducted using 230–400 mesh silica gel obtained from Dynamic Adsorbents, Inc. Melting points were obtained on a Thomas-Hoover apparatus and are uncorrected. Proton (400 MHz) and carbon (125 MHz) NMR spectra were recorded on a Bruker Avance III spectrometer in CDCl_3 unless otherwise noted. Chemical shifts are reported as δ units relative to internal tetramethylsilane. High resolution mass spectra were provided by the Washington University Mass Spectrometry Resource, St. Louis, MO. Each substrate that was evaluated for biological activity was >95% pure as determined by HPLC. All HPLC analyses were performed using a Hewlett Packard Model 1090 system with a YMC CombiScreen C18 column (50 × 4.6 mm). The solvent system was: solvent A (H_2O + 0.5% TFA); solvent B (CH_3CN + 0.1% TFA). Analyses were performed using a program of 10% solvent B for 1 min, a linear gradient of 10–90% solvent B over 10 min, 90% solvent B for 3 min, and then a linear gradient back to 10% solvent B over 5 min with a flow rate of 1.0 mL/min.

Nucleic Acid Molecules

The hTel DNA 24mer (5'-TTGGGTTAGGGTTAGGGTTAGGGA-3') was obtained in its HPLC-purified form from Integrated DNA Technologies, Inc. (Coralville, IA), while the AurA RNA 22mer (5'-AGGGGCGGCUGGUCGAGUGGC-3') was obtained in its PAGE-purified and desalted form from Dharmacon, Inc. (Chicago, IL). The concentrations of all AurA and hTel solutions were determined spectrophotometrically using the following extinction coefficients at 260 nm and 85 °C ($\epsilon_{260-85^\circ\text{C}}$) [in units of $(\text{mol strand/L})^{-1}\cdot\text{cm}^{-1}$]: 237,500 ± 4,700 for hTel and 236,200 ± 3,300 for AurA. These extinction coefficients were determined by enzymatic digestion and subsequent colorimetric phosphate assay using previously established protocols.²² Salmon testes (ST) duplex DNA, as well as the RNA polynucleotides, poly(rA) and poly(rU), were obtained from Sigma (St. Louis, MO), and used without further purification. Polynucleotide solution concentrations were determined using the following extinction coefficients in units of $(\text{mol nucleotide/L})^{-1}\cdot\text{cm}^{-1}$: $\epsilon_{258-25^\circ\text{C}} = 9,800$ for p(rA) and $\epsilon_{260-25^\circ\text{C}} = 9,350$ for p(rU).

General Method for Amide Formation. Method A: 2,6-Bis[[[1-(4-(methoxycarbonyl)oxazol-2-yl)-2-(triisopropylsilyloxy)ethyl]amino]carbonyl]pyridine (**3a**)

A solution of 2,6-pyridine dicarboxylic acid (418 mg, 2.5 mmol), **2** (1.71 g, 5 mmol), EDC (1.92g, 10 mmol) and HOBt (1.35 g, 10 mmol) in anhydrous DMF (100 mL) was treated with 2,6-lutidine (2.9 mL, 25 mmol) at 0 °C under argon. The reaction mixture was allowed to warm to room temperature overnight and was then concentrated under reduced pressure. The residue was taken up in a mixture of ethyl acetate and water and the layers were separated. The organic

layer was washed sequentially with 5% HCl, water, and brine and then dried over Na₂SO₄. Upon removal of the solvent and flash chromatography (15–50% EtOAc/hexanes) **3a** was obtained as a pale-yellow oil; 1.6 g (80% yield); ¹H NMR δ 8.54 (d, 2H, *J* = 8), 8.38 (d, 2H, *J* = 8), 8.24 (s, 2H), 8.04 (t, 1H, *J* = 7), 5.62 (dt, 2H, *J* = 6, 9), 4.26 (d, 4H, *J* = 7), 3.90 (s, 6H), 0.96 (m, 42H); ¹³C NMR δ 162.6, 162.4, 147.7, 143.2, 138.1, 132.6, 124.9, 122.4, 63.6, 51.2, 49.3, 16.9, 10.9.

2,6-Bis[[[1-(4-(methoxycarbonyl)oxazol-2-yl)-2-(triisopropylsilyloxy)ethyl]amino]carbonyl]-4-bromopyridine (**3b**)

Compound **3b** was prepared from **2** (2.86 g, 8.36 mmol) according to the procedure described for the synthesis of **3a** (method A) using **1b** (1.03 g, 4.18 mmol). Bis(amide) **3b** was obtained as a pale orange oil; 3.47 g (93% yield); ¹H NMR δ 8.50 (m, 4H), 8.24 (s, 2H), 5.59 (dt, 2H, *J* = 3, 6), 4.25 (d, 4H, *J* = 6), 3.85 (s, 6H), 0.90 (m, 42H); ¹³C NMR δ 162.1, 161.5, 156.2, 148.6, 143.3, 135.3, 132.6, 128.3, 63.4, 51.2, 49.4, 16.9, 11.0.

General Method for the Synthesis of Oxazoles. Method B: 2,6-Bis[4-[(4-methoxycarbonyl)oxazol-2-yl]oxazol-2-yl]pyridine (**4a**)

TIPS ether **3a** (750 mg, 0.92 mmol) was dissolved in a mixture of anhydrous THF (20 mL) and pyridine (2 mL) and HF-pyridine complex (0.5 mL) was added. The reaction was stirred at room temperature (drying tube) overnight and a white solid precipitated. A saturated aqueous solution of NaHCO₃ was added whereupon additional precipitate formed and was filtered. The solids were washed with water and the filtrate was then extracted with CH₂Cl₂. The organic phase was separated, dried over Na₂SO₄, and concentrated *in vacuo* to a white solid. This was combined with the filtered solid to give the diol as a white solid; 463 mg (100% yield); mp 218–220 °C; ¹H NMR (DMSO-*d*₆) δ 9.58 (d, 2H, *J* = 8), 8.84 (s, 2H), 8.24 (m, 3H), 5.29 (m, 2H), 4.04 (m, 4H), 3.79 (s, 6H); ¹³C NMR (DMSO-*d*₆) δ 163.3, 162.7, 160.9, 148.2, 145.4, 132.1, 125.1, 60.8, 51.6, 50.0; IR (Nujol) 3500, 3364, 3287, 1732 cm⁻¹.

The diol (463 mg, 0.92 mmol) was suspended in anhydrous CH₂Cl₂ (30 mL) and placed under argon. After cooling to –78 °C DAST (0.3 mL, 2.3 mmol) was added and the reaction was stirred for 4 hours at that temperature. Solid potassium carbonate (317 mg, 2.3 mmol) was added and the reaction mixture warmed slightly and was poured into saturated NaHCO₃ and extracted with CH₂Cl₂. The organic extracts were dried over Na₂SO₄ and concentrated under reduced pressure to give the bis(oxazoline) as a white solid; 428 mg (99.5% yield); mp 214–217 °C; ¹H NMR (CD₃OD) δ 8.36 (s, 2H), 8.26 (d, 2H, *J* = 8), 8.01 (t, 1H, *J* = 8), 5.67 (t, 2H, *J* = 9), 4.97 (d, 4H, *J* = 8), 4.28 (s, 6H); ¹³C NMR (CD₃OD) δ 165.5, 163.1, 161.5, 146.0, 145.1, 138.0, 133.3, 126.9, 71.4, 63.7, 52.1.

The bis(oxazoline) (428 mg, 0.92 mmol) was suspended in anhydrous CH₃CN (40 mL) and placed under argon. After cooling to 0 °C the magnetically-stirred solution was treated dropwise with DBU (0.55 mL, 3.68 mmol) and then BrCCl₃ (0.44 mL, 4.42 mmol). The reaction was allowed to warm to room temperature overnight and a white precipitate formed. The precipitate was filtered and washed with CH₂Cl₂ to give **4a** as a white solid; 341 mg (80% yield); mp >220 °C (dec.); ¹H NMR δ 8.59 (s, 2H), 8.44 (d, 2H, *J* = 8), 8.37 (s, 2H), 8.08 (t, 1H, *J* = 8), 3.98 (s, 6H).

2,6-Bis[4-[(4-methoxycarbonyl)oxazol-2-yl]oxazol-2-yl]-4-bromopyridine (**4b**)

Compound **4b** was prepared from **3b** using method B. Thus, **3b** (910 mg, 1.02 mmol) afforded 282 mg of **3b** (71% overall yield for the three steps) as a white solid; mp 280–282 °C (dec.); ¹H NMR δ 8.63 (s, 2H), 8.60 (s, 2H), 8.37 (s, 2H), 3.83 (s, 6H).

General Method for Ester Hydrolysis to Form Pyridyl Tetraoxazole Scaffolds. Method C: 2,6-Bis[4-(4-carboxyoxazol-2-yl)oxazol-2-yl]pyridine (5a)

Diester **4a** (150 mg, 0.32 mmol) was suspended in THF (50 mL) and H₂O (15 mL) and treated with LiOH (30 mg, 0.71 mmol). The mixture was heated to 80 °C overnight and was then cooled to room temperature. THF was removed by rotary evaporator and the residue was treated with 5% HCl. A white precipitate formed and was filtered and washed with water to give **5a** as a white solid; 140 mg (100% yield); mp 315–318 °C (dec.); ¹H NMR (DMSO-d₆) δ 9.00 (s, 2H), 8.52 (s, 2H), 8.15 (m, 3H); IR (Nujol) 3418–2719 (br), 1727 cm⁻¹.

2,6-Bis[4-(4-carboxyoxazol-2-yl)oxazol-2-yl]-4-bromopyridine (5b)

Compound **4b** (54 mg, 0.1 mmol) and LiBr (9 mg, 0.1 mmol) were suspended in THF (10 mL) and water (0.5 mL) and the mixture was then placed under argon. To this was added DBU (60 μL, 0.4 mmol) and the mixture was heated at reflux overnight. After cooling to room temperature solvents were removed under reduced pressure and the residue was treated with 1N HCl to give a white solid. This was filtered and washed with water and then CH₂Cl₂ to give **5b** as a white solid; 47 mg (100% yield); mp 205–206 °C (dec); ¹H NMR (DMSO) δ 9.19 (s, 2H), 8.90 (s, 2H), 8.48 (s, 2H); IR (thin film) 3390–2516 (br), 1727 cm⁻¹.

General Method for Macrocyclization. Method D: Pyridine tetraoxazole macrocycle with a 1,3-bis(aminomethyl)phenyl linker (6a)

Diacid **5a** (28 mg, 0.065 mmol), EDC (50 mg, 0.26 mmol) and HOBt (35 mg, 0.26 mmol) were dissolved in anhydrous DMF (120 mL) at room temperature under argon. The diamine linker, in this case 1,3-bis(aminomethyl)benzene (8.5 μL 0.065 mmol) in DMF (0.5 mL) and 2,6-lutidine (45 μL, 0.39 mmol) were added and the reaction was stirred at room temperature for 2 d. Solvent was removed under reduced pressure and the resulting residue was triturated with water. A white precipitate formed and was filtered, collected, and purified by flash chromatography eluting with 1–5% MeOH/CH₂Cl₂. Macrocycle **6a** was isolated as a white solid; 10 mg (30%), mp 320–324 °C (dec.); ¹H NMR (CDCl₃ + CD₃OD) δ 8.34 (d, 4H, *J* = 5), 8.11, (s, 3H), 7.58 (s, 1H), 7.33 (m, 3H), 4.62 (s, 4H); ¹³C NMR (CDCl₃ + CD₃OD) δ 159.8, 159.3, 153.3, 144.1, 140.5, 138.5, 138.0, 136.8, 136.6, 130.7, 129.3, 128.5, 128.1, 121.9, 42.8; HRMS (ESI) *m/z* calcd for C₂₇H₁₈N₇O₆ (M+H) 536.1368; found 536.1343.

4-Bromopyridine tetraoxazole macrocycle with a 1,3-bis(aminomethyl)phenyl linker (6b)

Using method D **5b** (43 mg, 0.1 mmol) was macrocyclized with 1,3-bis(aminomethyl)benzene (13 μL, 0.1 mmol). The product, **6b** was obtained as a white solid; 18 mg (35%); mp 211–213 °C; ¹H NMR (CDCl₃ + CD₃OD) δ 8.37 (s, 2H), 8.32 (m, 2H), 8.26 (s, 2H), 7.36 (s, 3H), 4.61 (s, 4H); ¹³C NMR (CDCl₃ + CD₃OD) δ 160.2, 159.7, 154.2, 146.1, 141.5, 139.8, 137.7, 137.4, 132.0, 130.2, 129.7, 129.4, 126.1, 108.0, 43.9; HRMS (ESI) *m/z* calcd for C₂₇H₁₇BrN₇O₆ (M+H): 614.0424; found: 614.0420.

Pyridine tetraoxazole macrocycle with a 2,6-bis(aminomethyl)pyridyl linker (7a)

Using method D **5a** (40 mg, 0.092 mmol) was macrocyclized with 2,6-bis(aminomethyl)pyridine¹⁵ (13 mg, 0.092 mmol). The product, **7a** was obtained as a white solid; 11 mg (22%); mp 330 °C (dec.); ¹H NMR (CDCl₃ + CD₃OD) δ 8.33 (s, 4H), 8.09 (s, 3H), 7.72 (t, 1H, *J* = 8), 7.40 (d, 2H, *J* = 8), 4.76 (s, 4H); ¹³C NMR (CDCl₃ + CD₃OD) δ 159.8, 159.5, 144.3, 140.4, 138.3, 137.8, 137.4, 136.4, 130.8, 122.5, 121.7, 71.2; HRMS (ESI) *m/z* calcd for C₂₆H₁₇N₈O₆ (M+H) 537.1271; found 537.1252.

General Method for Macrocyclization. Method E: Pyridine tetraoxazole macrocycle with a bis (2-aminoethyl)amine linker (8)

A solution of **5a** (23 mg, 0.053 mmol) and copper (II) triflate (19 mg, 0.053 mmol) in anhydrous DMF (100 mL) was stirred under argon at room temperature for 3 h. At that point EDC (41 mg, 0.21 mmol) and HOBt (29 mg, 0.21 mmol) were added and the color of the solution immediately became bright yellow. The solution was cooled to 0 °C and 2,6-lutidine (37 µL, 0.32 mmol) was added followed by a solution of diethylenetriamine (6 µL, 0.053 mmol) in 0.5 mL of DMF which was added by syringe pump over 30 minutes. The reaction was stirred at room temperature and the color gradually changed to pale blue. After 2 d solvent was removed under reduced pressure and the residue was triturated with water to give a white precipitate that was filtered and subjected to flash chromatography eluting with 1–5% MeOH/CH₂Cl₂ to give **8** as a white solid; 4 mg (15% yield); mp 276 °C (dec.); ¹H NMR (CDCl₃ + CD₃OD) δ 8.47 (s, 2H), 8.37 (s, 2H), 8.19 (s, 3H), 3.98 (m, 4H), 3.35 (m, 4H); HRMS (ESI) *m/z* calcd for C₂₃H₁₉N₈O₆ (M+H) 503.1428; found 503.1413.

2-[[[1-(4-(Methoxycarbonyl)oxazol-2-yl)-2-(triisopropylsilyloxy)ethyl]amino]thiocarbonyl]-6-[[[1-(4-(methoxycarbonyl)oxazol-2-yl)-2-(triisopropylsilyloxy)ethyl]amino]carbonyl]pyridine (9a)

A solution of **3a** (100 mg, 0.122 mmol) in toluene (10 mL) was treated with Lawesson's reagent (50 mg, 0.12 mmol) under argon and heated at 80 °C for 4 h. The reaction mixture was then allowed to cool to room temperature and toluene was removed by rotary evaporator. The residue was purified by flash chromatography eluting with 5–25% EtOAc/hexanes to afford **9a** as a yellow oil; 54 mg (53% yield); ¹H NMR δ 10.46 (d, 1H, *J* = 8), 8.82 (dd, 1H, *J* = 1, 9), 8.62 (d, 1H, *J* = 8), 8.36 (dd, 1H, *J* = 1, 8), 8.31 (s, 1H), 8.23 (s, 1H), 8.00 (t, 1H, *J* = 6), 6.19 (dt, 1H, *J* = 3, 5), 5.61 (dt, 1H, *J* = 2, 6), 4.38 (d, 2H, *J* = 5), 4.26 (d, 2H, 6), 3.88 (s, 6H), 0.95 (m, 42H); ¹³C NMR δ 190.7, 170.3, 162.7, 162.6, 161.6, 160.4, 146.5, 143.5, 143.2, 137.7, 133.0, 127.5, 124.6, 62.6, 54.7, 51.2, 49.4.

2,6-Bis[[[1-(4-(methoxycarbonyl)oxazol-2-yl)-2-(triisopropylsilyloxy)ethyl]amino]thiocarbonyl]-pyridine (9b)

A solution of **3a** (100 mg, 0.122 mmol) in toluene (10 mL) was treated with Lawesson's reagent (149 mg, 0.37 mmol) under argon and heated at 80 °C for 4 h. The reaction mixture was then allowed to cool to room temperature and toluene was removed by rotary evaporator. The residue was purified by flash chromatography eluting with 5–25% EtOAc/hexanes to afford **9b** as a yellow oil; 91 mg (88% yield); ¹H NMR δ 10.26 (d, 2H, *J* = 8), 8.79 (d, 2H, *J* = 8), 8.29 (s, 2H), 7.97 (t, 1H, *J* = 8), 6.18 (dt, 2H, *J* = 3, 6), 4.37 (m, 4H), 3.88 (s, 6H), 1.00 (m, 42H); ¹³C NMR δ 190.9, 161.5, 160.3, 148.7, 143.5, 137.4, 132.6, 127.1, 62.6, 54.7, 51.2, 16.8, 10.9.

2-[4-[(4-Methoxycarbonyl)oxazol-2-yl]thiazol-2-yl]-6-[4-[(4-methoxycarbonyl)oxazol-2-yl]oxazol-2-yl]pyridine (10a)

Compound **10a** was prepared from **9a** (138 mg, 0.166 mmol) using method B. The yield of **10a** for the three-step procedure was 57 mg (72%); cream-colored solid; mp 305–310 °C (dec.); ¹H NMR (CDCl₃ + CD₃OD) δ 8.62 (s, 1H), 8.49 (d, 1H, *J* = 7), 8.35 (m, 4H), 8.06 (m, 1H), 3.98 (s, 6H).

2,6-Bis[4-[(4-methoxycarbonyl)oxazol-2-yl]thiazol-2-yl]pyridine (10b)

Compound **10b** was prepared from **9b** (91 mg, 0.11 mmol) using method B. The yield of **10b** for the three-step procedure was 28 mg (52%); brown solid; mp 330–333 °C (dec.); ¹H NMR (DMSO-*d*₆) δ 9.10 (s, 2H), 8.80 (d, 2H, *J* = 8), 8.72 (s, 2H), 8.33 (t, 1H, *J* = 8), 3.93 (s, 6H).

Pyridine mono(thiazole) tris(oxazole) macrocycle with a 1,3-bis(aminomethyl)phenyl linker (11a)

Diester **10a** (57 mg, 0.12 mmol) was hydrolyzed to the corresponding diacid in 78% yield using method C. Macrocyclization of a portion of the diacid (23 mg, 0.051 mmol) with 1,3-bis(aminomethyl)benzene (7 μ L, 0.051 mmol) using method E afforded **11a** as white solid; 9 mg (33% yield); mp 245 °C; $^1\text{H NMR}$ δ 8.31 (s, 1H), 8.28 (s, 1H), 8.26 (s, 1H), 8.00 (m, 4H), 7.37 (m, 4H), 4.62, (m, 4H); $^{13}\text{C NMR}$ δ 140.0, 139.7, 138.4, 137.9, 136.7, 128.8, 128.3, 127.8, 127.4, 123.1, 121.9, 120.6, 113.4, 42.9, 42.3; HRMS (ESI) m/z calcd for $\text{C}_{27}\text{H}_{18}\text{N}_7\text{O}_5\text{S}$ (M+H): 552.1085; found: 552.1086.

Pyridine bis(thiazole) bis(oxazole) macrocycle with a 1,3-bis(aminomethyl)phenyl linker (11b)

Diester **10b** (52 mg, 0.11 mmol) was hydrolyzed to the corresponding diacid in quantitative yield using method C. A portion of the diacid (21 mg, 0.045 mmol) was dissolved in dry DMF (30 mL) and treated with EDC (17 mg, 0.09 mmol) and HOBt (12 mg, 0.09 mmol) and cooled to 0 °C under argon. To this was added 2,6-lutidine (26 μ L, 0.23 mmol) and 1-(N-Boc-aminomethyl)-3-(aminomethyl)benzene (11 μ L, 0.045 mmol) and the solution was allowed to warm to room temperature overnight. Solvents were removed under reduced pressure and the residue was extracted with EtOAc. The organic solution was washed with brine and dried over Na_2SO_4 , filtered, and evaporated to give 34 mg crude product. This was dissolved in CH_2Cl_2 (3 mL), cooled to 0 °C, and treated with TFA (3 mL). After stirring at 0 °C for 2 h solvents were removed under reduced pressure to give the free amine as its TFA salt (25 mg, 68% yield). Macrolactamization using method D gave product **11b** as white solid; 6 mg (43% yield); mp 274–275 °C (dec.); $^1\text{H NMR}$ ($\text{CDCl}_3 + \text{CD}_3\text{OD}$) δ 8.38 (m, 4H), 8.42 (s, 2H), 7.97 (m, 2H), 7.30 (m, 3H), 4.63 (d, 4H, $J = 6$); $^{13}\text{C NMR}$ ($\text{CDCl}_3 + \text{CD}_3\text{OD}$) δ 140.7, 137.4, 136.0, 128.4, 126.6, 126.5, 123.2, 120.5, 42.6; HRMS (ESI) m/z calcd for $\text{C}_{27}\text{H}_{18}\text{N}_7\text{O}_4\text{S}_2$ (M+H): 568.0863; found: 568.0864.

Pyridine tetraoxazole macrocycle with a 1,3-bis(aminomethyl)-5-bromophenyl linker (13a)

Using method D **5a** (43 mg, 0.1 mmol) was macrocyclized with 1-bromo-3,5-bis(aminomethyl)benzene dihydrochloride **12**¹⁷ (21 mg, 0.073 mmol). The product, **13a** was obtained as a white solid; 26 mg (58%); mp 248–250 °C; $^1\text{H NMR}$ δ 8.28 (s, 2H), 8.25 (s, 2H), 8.08 (m, 3H), 7.51 (m, 3H), 7.29 (m, 2H), 4.56 (d, 4H, $J = 5$); $^{13}\text{C NMR}$ δ 159.9, 159.3, 153.0, 144.3, 140.1, 138.5, 138.0, 136.7, 136.6, 130.7, 128.3, 126.0, 122.5, 42.9; HRMS (ESI) m/z calcd for $\text{C}_{27}\text{H}_{17}\text{BrN}_7\text{O}_6$ (M+H): 614.0418; found: 614.0418.

4-Bromopyridine tetraoxazole macrocycle with a 1,3-bis(aminomethyl)-5-bromophenyl linker (13b)

Using method D **5b** (17 mg, 0.033 mmol) was macrocyclized with **12** (10 mg, 0.033 mmol). The product, **13b** was obtained as a white solid; 5 mg (22%); mp 250 °C (dec); $^1\text{H NMR}$ ($\text{CDCl}_3 + \text{CD}_3\text{OD}$) δ 8.28 (s, 2H), 8.22 (s, 2H), 8.15 (s, 2H), 7.39 (s, 3H), 4.46 (s, 4H); $^{13}\text{C NMR}$ ($\text{CDCl}_3 + \text{CD}_3\text{OD}$) δ 160.3, 159.6, 145.7, 141.6, 139.8, 139.7, 131.7, 131.6, 128.4, 125.9, 122.7, 43.0; HRMS (ESI) m/z calcd for $\text{C}_{27}\text{H}_{16}\text{Br}_2\text{N}_7\text{O}_6$ (M+H): 691.9529; found: 691.9546.

5-[2-(Benzyloxycarbonylamino)ethyl]-1,3-bis[(*tert*-butyloxycarbonylamino)methyl]benzene (14a)

A solution of **12** (2.04 g, 9.5 mmol), di-*tert*-butyl dicarbonate (4.35 g, 19.9 mmol), and triethylamine (2.9 mL, 20.8 mmol) in anhydrous CH_2Cl_2 (25 mL) was stirred overnight under argon. The reaction mixture was poured 5% HCl and extracted with CH_2Cl_2 . The organic layer was dried over Na_2SO_4 , filtered and concentrated. Flash chromatography eluting with 10–40% EtOAc/hexanes gave the di-Boc derivative as a white solid; 2.51 g (63% yield); $^1\text{H NMR}$ δ

7.32 (s, 2H), 7.11 (s, 1H), 4.86 (s, 2H), 4.28 (d, 4H, $J = 4$), 1.46 (18H); ^{13}C NMR δ 154.8, 141.6, 129.2, 124.9, 122.9, 79.9, 44.0, 28.4.

A portion of the di-Boc derivative (209 mg, 0.5 mmol), potassium 2-(benzyloxycarbonylamino)ethyltrifluoroborate¹⁸ (186 mg, 0.76 mmol), Cs_2CO_3 (429 mg, 1.5 mmol), and $\text{PdCl}_2(\text{dppf})\cdot\text{CH}_2\text{Cl}_2$ (21 mg, 0.025 mmol) were dissolved in toluene (15 mL) and water (5 mL) was added. The flask was purged with argon and heated to 80 °C for 17.5 h. After cooling to room temperature the mixture was poured into saturated NH_4Cl and extracted with CH_2Cl_2 . The organic layer was dried over Na_2SO_4 , concentrated, and purified by flash chromatography eluting with 10–50% EtOAc/hexanes. The coupled product **14a** was obtained as a colorless oil; 205 mg (79% yield); ^1H NMR δ 7.32 (m, 5H), 7.04 (s, 1H), 6.98 (s, 2H), 5.09 (s, 2H), 4.82 (m, 3H), 4.26 (d, 4H, $J = 4$), 3.42 (m, 2H), 2.78 (m, 2H), 1.46 (s, 18H); ^{13}C -NMR δ 156.3, 155.9, 139.8, 139.5, 136.6, 128.5, 128.1, 126.8, 124.6, 79.6, 66.7, 44.5, 42.1, 36.0, 28.4.

5-[2-(Benzyloxycarbonylamino)ethyl]-1,3-bis(aminomethyl)benzene (**14b**)

A solution of **14a** (205 mg, 0.4 mmol) in CH_2Cl_2 (1 mL) and anisole (1 mL) and cooled to 0 °C. TFA (1 mL) was added and the solution was stirred at 0 °C for 3.75 h. The solution was evaporated under reduced pressure and residual anisole was removed azeotropically with benzene. The product was dissolved in MeOH and stirred for several minutes with IRA-400 resin. The resin was filtered and washed several times with MeOH. Upon evaporation of the solvent diamine **14b** was obtained as a white solid; 125 mg (100% yield); ^1H NMR δ 7.34 (m, 5H), 7.13 (s, 1H), 7.01 (s, 2H), 5.10 (s, 2H), 4.80 (s, 1H), 3.84 (s, 4H), 3.46 (m, 2H), 2.81 (m, 2H), 1.48 (br s, 4H); ^{13}C NMR δ 156.3, 144.0, 136.6, 128.5, 128.2, 126.0, 124.1, 66.7, 46.4, 42.2, 36.1.

Pyridine tetraoxazole macrocycle with a 5-[2-(benzyloxycarbonylamino)ethyl]-1,3-bis(aminomethyl)phenyl linker (**15a**)

Using method D **5a** (50 mg, 0.11 mmol) was macrocyclized with **14b** (36 mg, 0.11 mmol). The product, **15a** was obtained as a white solid; 33 mg (42%); mp 196–198 °C; ^1H NMR ($\text{CDCl}_3 + \text{CD}_3\text{OD}$) δ 8.41 (d, 2H, $J = 4$), 8.34 (s, 2H), 8.32 (s, 2H), 8.10 (s, 3H), 7.42 (s, 1H), 7.30 (m, 5H), 7.18 (s, 2H), 5.37 (s, 1H), 5.04 (s, 2H), 4.59 (d, 4H, $J = 4$), 3.41 (m, 4H); ^{13}C NMR ($\text{CDCl}_3 + \text{CD}_3\text{OD}$) δ 160.9, 160.4, 156.8, 156.7, 154.3, 145.1, 141.5, 140.4, 139.5, 139.0, 138.1, 137.6, 136.8, 131.7, 129.6, 128.5, 128.2, 128.0, 127.9, 122.9, 66.6, 42.2, 35.9; HRMS (ESI) m/z calcd for $\text{C}_{37}\text{H}_{29}\text{N}_8\text{O}_8$ (M+H): 713.2108; found: 713.2091.

4-Bromopyridine tetraoxazole macrocycle with a 5-[2-(benzyloxycarbonylamino)ethyl]-1,3-bis(aminomethyl)phenyl linker (**15b**)

Using method D **5b** (20 mg, 0.039 mmol) was macrocyclized with **14b** (12 mg, 0.039 mmol). The product, **15b** was obtained as a white solid; 13 mg (42%); mp 204–205 °C; ^1H NMR δ 8.24 (m, 5H), 7.65 (s, 2H), 7.56 (m, 2H), 7.3 (m, 5H), 7.17 (s, 2H), 5.06 (s, 2H), 4.91 (s, 1H), 4.56 (s, 2H), 3.44 (m, 2H), 2.80 (m, 2H); ^{13}C NMR δ 159.6, 159.4, 159.4, 156.3, 154.0, 153.9, 147.6, 146.2, 140.8, 139.4, 138.1, 137.5, 136.7, 134.9, 132.1, 132.0, 130.0, 129.9, 128.5, 128.4, 128.3, 127.9, 127.7, 125.9, 125.9, 121.1, 108.2, 107.8, 66.5, 43.8, 42.2, 35.9; HRMS (ESI) m/z calcd for $\text{C}_{37}\text{H}_{28}\text{BrN}_8\text{O}_8$ (M+H): 791.1213; found: 791.1199.

N-(3,5-Bis(aminomethyl)phenethyl)-2,2,2-trifluoroacetamide (**16**)

A solution of **14a** (62 mg, 0.13 mmol) in EtOH (10 mL) was treated with 20% $\text{Pd}(\text{OH})_2/\text{C}$ (10 mg) and stirred under 1 atm H_2 (balloon) for 21 h. The catalyst was filtered and washed with EtOH to afford the primary phenethylamine as a colorless oil; 50 mg (100% yield); ^1H NMR

δ 7.02 (m, 3H), 4.94 (s, 2H), 4.27 (d, 4H, $J = 8$), 2.94 (m, 2H), 2.71 (m, 2H), 1.47 (s, 18H); ^{13}C NMR δ 155.9, 140.7, 139.6, 126.9, 124.3, 79.5, 44.5, 43.4, 39.9, 28.4.

A portion of the amine (37 mg, 0.097 mmol) was dissolved in a solution of pyridine (3 mL) and trifluoroacetic anhydride (2 mL) and stirred at room temperature under a drying tube for 19 h. The reaction mixture was diluted with CH_2Cl_2 and washed with 5% HCl. The aqueous layer was back-extracted with CH_2Cl_2 (3 \times 20 mL) and the combined organic layers were washed with 5% HCl and then dried over Na_2SO_4 . After concentration, flash chromatography (10–40% EtOAc/hexanes) afforded the trifluoroacetamide as a pale-yellow oil; 42 mg (91% yield); ^1H NMR δ 7.06 (s, 1H), 6.98 (s, 2H), 6.82 (s, 1H), 4.96 (s, 2H), 4.25 (d, 4H, $J = 8$), 3.55 (m, 2H), 2.84 (m, 2H), 1.46 (s, 18H); ^{13}C NMR δ 157.8, 157.5, 157.1, 156.7, 156.0, 140.1, 138.6, 126.7, 124.9, 117.3, 114.4, 79.7, 44.4, 40.9, 34.8, 28.4.

The Boc groups were removed by dissolving the trifluoroacetamide (63 mg, 0.13 mmol) in dry CH_2Cl_2 (2 mL), cooling to 0 °C under argon, and adding TFA (1 mL). After 1.5 h solvent was removed under reduced pressure to give **16** as a pale-yellow oil; 65 mg (100% yield); ^1H NMR δ 7.34 (s, 1H), 7.31 (s, 2H), 5.92 (s, 1H), 4.00 (s, 4H), 3.54 (m, 2H), 2.88 (m, 2H); ^{13}C NMR δ 139.9, 137.3, 128.5, 126.0, 47.8, 43.6, 32.8.

Pyridine tetraoxazole macrocycle with a 5-[2-(trifluoroacetamido)ethyl]-1,3-bis(aminomethyl)phenyl linker (**17**)

Using method D **5a** (44 mg, 0.1 mmol) was macrocyclized with **16** (51 mg, 0.1 mmol). The product, **17** was obtained as a white solid; 21 mg (31% yield); mp 290 °C (dec.); ^1H NMR ($\text{CDCl}_3 + \text{CD}_3\text{OD}$) δ 8.38 (s, 2H), 8.37 (s, 2H), 8.12 (s, 2H), 7.60 (s, 1H), 7.47 (s, 1H), 7.19 (s, 2H), 4.60 (s, 4H), 4.07 (m, 2H), 3.40 (m, 2H); ^{13}C NMR ($\text{CDCl}_3 + \text{CD}_3\text{OD}$) δ 160.9, 154.1, 145.0, 141.6, 140.0, 139.5, 138.2, 137.6, 131.6, 129.7, 128.6, 122.9, 43.7, 38.8, 34.1; HRMS (ESI) m/z calcd for $\text{C}_{31}\text{H}_{22}\text{F}_3\text{N}_8\text{O}_7$ (M+H): 675.1564; found: 675.1564.

Pyridine tetraoxazole macrocycle with a 5-(2-aminoethyl)-1,3-bis(aminomethyl)phenyl linker (**18**)

A suspension of **17** (15 mg, 0.02 mmol) and K_2CO_3 (17 mg, 0.12 mmol) in MeOH (10 mL) was heated at reflux for 4.75 h. After cooling to room temperature solvent was removed under reduced pressure and the residue was partitioned between water and CH_2Cl_2 . The organic layer was separated and dried over Na_2SO_4 , filtered, and evaporated to give **18** as a white solid; 10.5 mg (81% yield); mp 277–280 °C (dec.); ^1H NMR ($\text{CDCl}_3 + \text{CD}_3\text{OD}$) δ 8.42 (s, 2H), 8.40 (s, 2H), 8.13 (s, 3H), 7.45 (s, 1H), 7.19 (s, 2H), 4.60 (s, 4H), 2.92 (m, 2H), 2.75 (m, 2H); ^{13}C NMR ($\text{CDCl}_3 + \text{CD}_3\text{OD}$) δ 161.0, 160.5, 154.4, 145.1, 141.7, 140.9, 139.7, 139.2, 138.1, 137.6, 131.7, 129.5, 129.2, 128.9, 123.0, 43.8, 43.0, 39.4; HRMS (ESI) m/z calcd for $\text{C}_{29}\text{H}_{23}\text{N}_8\text{O}_6$ (M+H): 579.1741; found: 579.1723.

Pyridine tetraoxazole macrocycle with a 5-[2-(N,N-dimethylamino)ethyl]-1,3-bis(aminomethyl)phenyl linker (**19**)

Primary amine **18** (6 mg, 0.01 mmol) was dissolved in 1:4 MeOH/ CH_2Cl_2 (5 mL) and placed under argon. A solution of 37% aqueous formaldehyde (0.25 mL) was added the reaction mixture was allowed to stir at room temperature for 10 min. At that point sodium triacetoxyborohydride (15 mg, 0.07 mmol) was added and stirring continued for 16 h. The reaction was not complete by TLC and additional formaldehyde solution (0.25 mL) and $\text{NaBH}(\text{OAc})_3$ (15 mg) was added. After 6 h TLC showed the reaction to be complete and it was poured into saturated NaHCO_3 and extracted with CH_2Cl_2 . After concentrating, flash chromatography (1–15% MeOH/ CH_2Cl_2) afforded **19** as a white solid; 6 mg (100% yield); 295 °C (dec.); ^1H NMR ($\text{CDCl}_3 + \text{CD}_3\text{OD}$) δ 8.34 (s, 2H), 8.33 (s, 2H), 8.10 (s, 3H), 7.41 (s, 1H), 7.19 (s, 2H), 4.59 (s, 4H), 2.79 (m, 2H), 2.61 (m, 2H), 2.30 (s, 6H); ^{13}C NMR ($\text{CDCl}_3 +$

CD₃OD) δ 160.8, 160.3, 154.2, 145.1, 141.5, 139.4, 139.0, 137.9, 131.7, 129.4, 128.1, 122.8, 45.0, 43.8; HRMS (ESI) m/z calcd for C₃₁H₂₇N₈O₆ (M+H): 607.2054; found: 607.2029.

2,6-Bis[[[1-(4-(methoxycarbonyl)oxazol-2-yl)-2-(triisopropylsilyloxy)ethyl]amino]carbonyl]-4-hydroxypyridine (20)

Using method A chelidonic acid (230 mg, 1.26 mmol) was condensed with **2** (860 mg, 2.51 mmol). The product, **20** was obtained as a yellow oil; 900 mg (86% yield); ¹H NMR δ 10.62 (s, 1H), 8.70 (d, 2H, $J = 9$), 8.25 (s, 2H), 7.82 (s, 2H), 5.57 (m, 2H), 4.24 (d, 4H, $J = 6$), 3.90 (s, 6H), 0.96 (m, 42H); ¹³C NMR δ 165.9, 163.0, 162.0, 160.4, 149.2, 143.2, 132.4, 112.6, 63.5, 51.2, 49.2, 16.8, 10.9.

2,6-Bis[[[1-(4-(methoxycarbonyl)oxazol-2-yl)-2-(triisopropylsilyloxy)ethyl]amino]carbonyl]-4-[(3-phthalimidopropyl)oxy]pyridine (21)

A solution of **20** (642 mg, 0.77 mmol) and N-(3-bromopropyl)phthalimide (227 mg, 0.85 mmol) in anhydrous DMF (10 mL) was treated with DBU (0.13 mL, 0.85 mmol) and warmed to 60 °C for 6 h. After cooling to room temperature the reaction mixture was poured into water and extracted with EtOAc. The organic phase was washed with 5% HCl and then brine and then dried over Na₂SO₄. Flash chromatography (1–4% MeOH/CH₂Cl₂) afforded **21** as a colorless oil; 727 mg (92% yield); ¹H NMR δ 8.61 (d, 2H, $J = 9$), 8.24 (s, 2H), 7.84 (m, 2H), 7.73 (m, 4H), 5.59 (m, 2H), 4.23 (m, 6H), 3.93 (m, 8H), 2.25 (m, 2H), 1.03 (m, 42H); ¹³C NMR δ 167.4, 166.4, 162.5, 162.3, 160.5, 149.5, 143.3, 133.2, 132.6, 131.2, 122.5, 111.1, 65.7, 63.5, 51.2, 49.3, 34.2, 27.0, 16.9, 10.9.

2,6-Bis[4-(4-carboxyoxazol-2-yl)oxazol-2-yl]-4-[(3-phthalimidopropyl)oxy]pyridine (22)

Using method B, **21** (1.05 g, 1.03 mmol) was deprotected, cyclodehydrated, and converted into the pyridyl tetraoxazole diester, a white solid; 470 mg (68% yield for the three steps); ¹H NMR (DMSO-*d*₆) δ 9.16 (s, 2H), 9.02 (s, 2H), 7.82 (m, 4H), 7.61 (s, 2H), 4.37 (t, 2H, $J = 6$), 3.81 (t, 2H, $J = 6$), 2.14 (m, 2H).

A portion of this material (150 mg, 0.23 mmol) was dissolved in DMF (5 mL) and treated with LiCl (95 mg, 2.3 mmol) at reflux overnight. After cooling to room temperature DMF was removed under reduced pressure. Addition of 1N HCl to the residue formed a precipitate that was filtered and washed with water to give **22** as a white solid; 144 mg (100% yield); mp 147–150 °C; ¹H NMR (DMSO-*d*₆) δ 9.14 (s, 2H) 8.90 (s, 2H), 7.82 (m, 4H), 7.62 (s, 2H), 4.37 (t, 2H, $J = 6$), 3.81 (t, 2H, $J = 6$), 2.14 (m, 2H).

4-[(3-Phthalimidopropyl)oxy]pyridine tetraoxazole macrocycle with a 1,3-bis(aminomethyl) phenyl linker (23a)

Using method D **22** (45 mg, 0.071 mmol) was macrocyclized with 1,3-bis(aminomethyl) benzene (9 μ L, 0.071 mmol). The product, **23b** was obtained as a white solid; 18 mg (35%); mp 249–252 °C (dec.); ¹H NMR δ 8.24 (s, 2H), 8.23 (s, 2H), 7.85 (dd, 2H, $J = 3, 5$), 7.72 (dd, 2H, $J = 3, 5$), 7.49 (m, 4H), 7.37 (m, 4H), 4.59 (d, 4H, $J = 5$), 4.27 (t, 2H, $J = 6$), 3.97 (t, 2H, $J = 6$), 2.30 (dt, 2H, $J = 6, 12$); ¹³C NMR δ 168.4, 166.7, 160.5, 159.7, 154.3, 146.8, 140.5, 138.8, 137.8, 137.5, 134.1, 132.1, 131.9, 129.9, 129.9, 129.5, 123.4, 109.4, 66.7, 43.9, 35.1, 28.0; HRMS (ESI) m/z calcd for C₃₈H₂₇N₈O₉ (M+H): 739.1896; found: 739.1891.

4-[(3-Phthalimidopropyl)oxy]pyridine tetraoxazole macrocycle with a 1,3-bis(aminomethyl)-5-bromophenyl linker (23b)

Using method D **22** (22 mg, 0.034 mmol) was macrocyclized with **12** (10 mg, 0.034 mmol). The product, **23b** was obtained as a white solid; 8.3 mg (30%); mp 289–290 °C (dec.); ¹H NMR (CDCl₃ + CD₃OD) δ 8.33 (s, 4H), 7.86 (dd, 2H, $J = 3, 5$), 7.75 (dd, 2H, $J = 3, 5$), 7.51

(m, 5H), 4.58 (s, 4H), 4.29 (t, 2H, $J = 6$), 3.98 (t, 2H, $J = 7$), 2.31 (dt, 2H, $J = 6, 12$); ^{13}C NMR ($\text{CDCl}_3 + \text{CD}_3\text{OD}$) δ 168.6, 167.2, 160.9, 160.5, 154.3, 146.4, 141.6, 139.9, 139.3, 137.5, 134.4, 132.1, 131.9, 131.6, 128.7, 123.5, 122.8, 109.5, 66.9, 43.2, 35.1, 28.0; HRMS (ESI) m/z calcd for $\text{C}_{38}\text{H}_{26}\text{BrN}_8\text{O}_9$ (M+H): 817.1006; found: 817.0986.

4-[(3-Phthalimidopropyl)oxy]pyridine tetraoxazole macrocycle with a 5-[2-(benzyloxycarbonylamino)ethyl-1,3-bis(aminomethyl)-5-bromophenyl linker (23c)

Using method D **22** (21 mg, 0.033 mmol) was macrocyclized with **14b** (15 mg, 0.048 mmol). The product, **23c** was obtained as a white solid; 11 mg (40%); mp 167–170 °C; ^1H NMR δ 8.24 (s, 2H), 8.23 (s, 2H), 7.85 (dd, 2H, $J = 3,5$), 7.72 (dd, 2H, $J = 3,5$), 7.56 (m, 2H), 7.47 (s, 2H), 7.27 (m, 5H), 7.17 (s, 3H), 5.04 (s, 2H), 4.95 (m, 1H), 4.56 (d, 4H, $J = 4$), 4.27 (t, 2H, $J = 6$), 3.97 (t, 2H, $J = 6$), 3.45 (m, 2H), 2.81 (m, 2H), 2.32 (dt, 2H, $J = 6, 12$); ^{13}C NMR δ 168.4, 166.8, 160.5, 159.7, 156.3, 154.2, 146.7, 140.6, 138.8, 138.1, 137.4, 134.1, 132.1, 131.8, 130.0, 129.1, 128.4, 128.3, 128.2, 127.9, 125.3, 123.4, 109.4, 66.7, 43.8, 35.0, 28.0; HRMS (ESI) m/z calcd for $\text{C}_{48}\text{H}_{38}\text{N}_9\text{O}_{11}$ (M+H): 916.2691; found: 916.2669.

4-[(3-Aminopropyl)oxy]pyridine tetraoxazole macrocycle with a 1,3-bis(aminomethyl)phenyl linker (23d)

Hydrazine monohydrate (0.5 mL, 10.3 mmol) was added to a solution of **23a** (24 mg, 0.033 mmol) in EtOH (10 mL). The solution was heated at reflux for 3 h, cooled to room temperature, and concentrated under reduced pressure. The residue was dissolved in CH_2Cl_2 , washed with 10% NaOH, and dried over Na_2SO_4 . Evaporation of the solvent afforded **23d** as a white solid; 20 mg (100% yield); mp 237–239 °C (dec.); ^1H NMR ($\text{CDCl}_3 + \text{CD}_3\text{OD}$) δ 8.32 (m, 4H), 7.57 (s, 3H), 7.36 (m, 3H), 4.63 (s, 4H), 4.27 (m, 2H), 2.94 (t, 2H, $J = 6$), 2.04 (dt, 2H, $J = 6, 12$); ^{13}C NMR ($\text{CDCl}_3 + \text{CD}_3\text{OD}$) δ 167.4, 160.9, 160.3, 154.3, 146.4, 141.4, 139.4, 137.8, 137.5, 131.6, 130.2, 129.5, 129.2, 109.6, 66.7, 43.8, 38.4, 32.0; HRMS (ESI) m/z calcd for $\text{C}_{30}\text{H}_{25}\text{N}_8\text{O}_7$ (M+H): 609.1846; found: 609.1825.

Cytotoxicity assays

Cytotoxicity was determined using the MTT-microtiter plate tetrazolinium assay (MTA). The human lymphoblast RPMI 8402 cell line was provided by Dr. Toshiwo Andoh (Aichi Cancer Center Research Institute, Nagoya, Japan).²³ The KB3-1 cell line and its multidrug-resistant variant KBV-1 were obtained from K.V. Chin (The Cancer Institute of New Jersey, New Brunswick, NJ).²⁴ The KBH5.0 cell line was derived from KB3-1 by stepwise selection against Hoechst 33342.²⁵ The cytotoxicity assay was performed using 96-well microtiter plates. Cells were grown in suspension at 37 °C in 5% CO_2 and maintained by regular passage in RPMI medium supplemented with 10% heat inactivated fetal bovine serum, L-glutamine (2 mM), penicillin (100 U/mL), and Streptomycin (0.1 mg/mL). For determination of IC_{50} values, cells were exposed continuously for four days to varying concentrations of drug, and MTT assays were performed at the end of the fourth day. Each assay was performed with a control that did not contain any drug. All assays were performed at least twice in six replicate wells.

Temperature-Dependent Spectrophotometry

Temperature-dependent absorption experiments were conducted on an AVIV Model 14DS Spectrophotometer (Aviv Biomedical, Lakewood, NJ) equipped with a thermoelectrically controlled cell holder. Quartz cells with a pathlength of 1.0 cm were used for all the absorbance studies. Temperature-dependent absorption profiles were acquired at either 260 nm (for ST duplex DNA and poly(rA)•poly(rU) duplex RNA) or 295 nm (for hTel quadruplex DNA and AurA quadruplex RNA) with a 7 sec averaging time. The temperature was raised in 0.5 °C increments, and the samples were allowed to equilibrate for 1 min at each temperature setting. In the quadruplex melting studies, the hTel and AurA concentrations were 5 μM in strand.

When present in these quadruplex studies, the drug concentrations were 20 μM . In the duplex melting studies, the ST DNA concentrations were 30 μM base pair, while the poly(rA)•poly(rU) concentrations were 15 μM base pair. When present, the drug concentrations were 15 μM in the ST DNA studies and 7.5 μM in the poly(rA)•poly(rU) studies. The buffer for all the UV melting experiments contained 10 mM potassium phosphate (pH 7.5) and sufficient KCl (132 mM) to bring the total K^+ concentration to 150 mM. Prior to their use in the UV melting experiments, all nucleic acid solutions were preheated at 90 °C for 5 min and slowly cooled to room temperature over a period of 4 hr.

Human tumor xenograft assay

Bioassays were performed using female NCR/NU NU mice of approximately 9 weeks of age as obtained from Taconic Farms, Inc. (Germantown, NY, USA). Mice were housed 3–4 per cage in laminar flow HEPA filtered microisolator caging (Allentown Caging Equipment Co., Allentown, NJ, USA). Mice were fed Purina autoclavable breeder chow #5021 and given drinking water, purified by reverse-osmosis, *ad libitum*. Five days after arrival within the animal facility, the mice were inoculated on the right flank with 1.5×10^6 MDA-MB-435 tumor cells in 0.1 mL of RPMI 1640 Media by sc injection (25 gauge needle \times 5/8"). The MDA-MB-435 cells were grown in 75 cm^2 flasks using RPMI 1640 Media and 10% fetal bovine serum. Tumors were of sufficient size at 19–20 days after inoculation. Tumor-bearing mice were evenly matched in each experimental group based on tumor volume. Mice were injected ip 3 \times weekly on alternate days. Negative controls consisted of seven mice that received 150 μl of 10 mM citrate. The positive control group consisted of eight mice that received irinotecan (CPT-11, Camptosar®) by ip injection at a dose of 20 mg/kg, 3 \times weekly, for all four weeks. Compound **19** was similarly administered to seven mice, 3 \times weekly, at doses of 0, 25, 32 and 42 mg/kg for weeks 1–4, respectively. Tumor volume was calculated by measuring the tumor with a microcaliper. The length (l) is the maximum two dimensional distance of the tumor and the width (w) is the maximum distance perpendicular to this length measured in mm. Tumor volume was calculated using the formula $(l \times w^2)/2$. Body weights and tumor volumes of individual mice were determined at a minimum of twice a week.

Acknowledgments

Financial support for this research was provided by Department of Defense Grant W81XWH06-1-0514. The Bruker Avance III 400 NMR spectrometer used for this study was purchased with funds from NCR Grant No. 1S10RR23698-1A1. Mass spectrometry was provided by the Washington University Mass Spectrometry Resource with support from the NIH National Center for Research Resources (Grant No. P41RR0954).

Abbreviations

Boc	<i>tert</i> -butoxycarbonyl
Cbz	benzyloxycarbonyl
DAST	(diethylamino)sulfur trifluoride
DBU	1,8-diazabicyclo[5.4.0]undec-7-ene
DMF	N,N-dimethylformamide
EDC	N-(3-dimethylaminopropyl)-N'-ethylcarbodiimide
HOBt	1-hydroxybenzotriazole
HXDV	hexaoxazole divalene
TFA	trifluoroacetic acid
TFAA	trifluoroacetic anhydride

TIPS triisopropylsilyl

References

1. (a) Han H, Hurley LH. G-Quadruplex DNA: a potential target for anti-cancer drug design. *TiPS* 2000;21:136–142. [PubMed: 10740289] (b) Hurley LH, Wheelhouse RT, Sun D, Kerwin SM, Salazar M, Fedoroff OY, Han FX, Han H, Izbicka E, Von Hoff DD. G-Quadruplexes as targets for drug design. *Pharmacol Therap* 2000;85:141–158. [PubMed: 10739869] (c) Neidle S, Read MA. G-Quadruplexes as therapeutic targets. *Biopolymers* 2001;56:195–208. [PubMed: 11745111]
2. Shin-ya K, Wierzba K, Matsuo K-i, Ohtani T, Yamada Y, Furihata K, Hayakawa Y, Seto H. Telomestatin, a novel telomerase inhibitor from *Streptomyces anulatus*. *J Am Chem Soc* 2001;123:1262–1263. [PubMed: 11456694]
3. Kim M-Y, Vankayalapati H, Shin-ya K, Wierzba K, Hurley LH. Telomestatin, a potent telomerase inhibitor that interacts quite specifically with the human telomeric intramolecular G-quadruplex. *J Am Chem Soc* 2002;124:2098–2099. [PubMed: 11878947]
4. Tahara H, Shin-ya K, Seimiya H, Yamada H, Tsuruo T, Ide T. G-Quadruplex stabilization by telomestatin induces TRF2 protein dissociation from telomeres and anaphase bridge formation accompanied by loss of the 3' telomeric overhang in cancer cells. *Oncogene* 2006;25:1955–1966. [PubMed: 16302000]
5. For representative examples see: (a) Sun D, Thompson B, Cathers BE, Salazar M, Kerwin SM, Trent JO, Jenkins TC, Neidle S, Hurley LH. Inhibition of human telomerase by a G-quadruplex-interactive compound. *J Med Chem* 1997;40:2113–2116. [PubMed: 9216827] (b) Wheelhouse RT, Sun D, Han H, Han FX, Hurley LH. Cationic porphyrins as telomerase inhibitors: The interaction of tetra-(N-methyl-4-pyridyl)porphine with quadruplex DNA. *J Am Chem Soc* 1998;120:3261–3262. (c) Fedoroff OY, Salazar M, Han H, Chemeris VV, Kerwin SM, Hurley LH. NMR-Based model of a telomerase-inhibiting compound bound to G-quadruplex DNA. *Biochemistry* 1998;37:12367–12374. [PubMed: 9730808] (d) Harrison RJ, Gowan SM, Kelland LR, Neidle S. Human telomerase inhibition by substituted acridine derivatives. *Bioorg Med Chem Lett* 1999;9:2463–2468. [PubMed: 10498189] (e) Koeppel F, Riou JF, Laoui A, Mailliet P, Arimondo PB, Labit D, Petitgenet O, Hélène C, Mergny JL. Ethidium derivatives bind to G-quartets, inhibit telomerase and act as fluorescent probes for quadruplexes. *Nucl Acids Res* 2001;29:1087–1096. [PubMed: 11222758] (f) Duan W, Rangan A, Vankayalapati H, Kim MY, Zeng Q, Sun D, Han H, Fedoroff OY, Nishioka D, Rha SY, Izbicka E, Von Hoff DD, Hurley LH. Design and synthesis of fluoroquinophenoxazines that interact with human telomeric G-quadruplexes and their biological effects. *Mol Cancer Therap* 2001;1:103–120. [PubMed: 12467228]
6. (a) Perry PJ, Jenkins TC. DNA tetraplex-binding drugs: structure-selective targeting is critical for antitumour telomerase inhibition. *Mini Rev Med Chem* 2001;1:31–41. [PubMed: 12369989] (b) Yu H, Wang X, Fu M, Ren J, Qu X. Chiral metallo-supramolecular complexes selectively recognize human telomeric G-quadruplex DNA. *Nucl Acids Res* 2008;36:5695–5703. [PubMed: 18776218] (c) Yu H, Zhao C, Chen Y, Fu M, Ren M, Qu X. DNA loop sequence as the determinant for chiral supramolecular compound G-quadruplex selectivity. *J Med Chem* 2010;53:492–498. [PubMed: 19911822]
7. (a) Minhas GS, Pilch DS, Kerrigan JE, LaVoie EJ, Rice JE. Synthesis and G-quadruplex stabilizing properties of a series of oxazole-containing macrocycles. *Bioorg Med Chem Lett* 2006;16:3891–3895. [PubMed: 16735121] (b) Satyanarayana M, Rzuczek SG, LaVoie EJ, Pilch DS, Liu A, Liu LF, Rice JE. Ring-closing metathesis for the synthesis of a highly G-quadruplex selective macrocyclic hexaoxazole having enhanced cytotoxic potency. *Bioorg Med Chem Lett* 2008;18:3802–3804. [PubMed: 18515097] (c) Barbieri CM, Srinivasan AR, Rzuczek SG, Rice JE, LaVoie EJ, Pilch DS. Defining the mode, energetics and specificity with which a macrocyclic hexaoxazole binds to human telomeric G-quadruplex DNA. *Nucl Acids Res* 2007;35:3272–3286. [PubMed: 17452355] LaVoie, EJ.; Kim, YA.; Satyanarayana, M.; Rzuczek, SG.; Pilch, DS.; Tsai, Y-C.; Qi, H.; Lin, C-P.; Liu, A.; Liu, LF.; Rice, JE. Oxazole-containing macrocycles as selective G-quadruplex stabilizers. *Mol. Targets Cancer Therap. Proc*; Nov. 2009; Boston, MA. p. 275

8. (a) Binz N, Shalaby T, Rivera P, Shin-ya K, Grotzer MA. Telomerase inhibition, telomere shortening, cell growth suppression and induction of apoptosis by telomestatin in childhood neuroblastoma cells. *Eur J Cancer* 2005;41:2873–2881. [PubMed: 16253503] (b) Liu W, Sun D, Hurley LH. Binding of G-quadruplex-interactive agents to distinct G-quadruplexes induces different biological effects in MiaPaCa cells. *Nucleos Nucleot Nucl* 2005;24:1801–1815.
9. Tsai YC, Qi H, Lin CP, Lin RK, Kerrigan JE, Rzuczek SG, LaVoie EJ, Rice JE, Pilch DS, Lyu YL, Liu LF. A G-Quadruplex stabilizer induces M phase cell cycle arrest. *J Biol Chem* 2009;284:22535–22543. [PubMed: 19531483]
10. (a) Rzuczek SG, Pilch DS, LaVoie EJ, Rice JE. Lysinyl macrocyclic hexaoxazoles: Synthesis and selective G-quadruplex stabilizing properties. *Bioorg Med Chem Lett* 2008;18:913–917. [PubMed: 18248989] (b) Pilch DS, Barbieri CM, Rzuczek SG, LaVoie EJ, Rice JE. Targeting human telomeric G-quadruplex DNA with oxazole-containing macrocyclic compounds. *Biochimie* 2008;90:1233–1249. [PubMed: 18439430]
11. Philips AJ, Uto Y, Wipf P, Reno MJ, Williams DR. Synthesis of functionalized oxazolines and oxazoles with DAST and Deoxo-Fluor. *Org Lett* 2000;2:1165–1168. [PubMed: 10804580]
12. Williams DR, Lowder PD, Gu YG, Brooks DA. Studies of mild dehydrogenations in heterocyclic systems. *Tetrahedron Lett* 1997;38:331–334.
13. Pryor KE, Shippy GW Jr, Skyler DA, Rebek J Jr. The activated core approach to combinatorial chemistry: A selection of new core molecules. *Tetrahedron* 1998;54:4107–4124.
14. Seebach D, Thaler A, Blaser A, Ko SY. Transesterifications with 1,8-diazabicyclo[5.4.0]undec-7-ene/lithium bromide (DBU/LiBr) – also applicable to cleavage of peptides from resins in Merrifield syntheses. *Helv Chim Acta* 1991;74:1102–1118.
15. Shibatomi K. Preparation of optically active 2,6-bis(aminomethyl)pyridines and asymmetric reactions with their metal complex catalysts. *Jpn Kokai Tokkyo Koho*. 2008 JP 2008024596 A 20080207.
16. Fritz H, Hug P, Lawesson SO, Logemann E, Pedersen BS, Sauter H, Scheibye S, Winkler T. Studies on organophosphorus compounds. XXVI. Synthesis and carbon-13 NMR spectra of N,N-dialkyl thioamides. *Bull Soc Chim Belg* 1978;87:525–534.
17. Manabe K. Synthesis of novel chiral quaternary phosphonium salts with a multiple hydrogen-bonding site, and their application to asymmetric phase-transfer alkylation. *Tetrahedron* 1998;54:14465–14476.
18. (a) Molander GA, Vargas F. β -Aminoethyltrifluoroborates: Efficient aminoethylations *via* Suzuki-Miyaura cross-coupling. *Org Lett* 2007;9:203–206. [PubMed: 17217265] (b) Molander GA, Jean-Gérard L. Scope of the Suzuki-Miyaura aminoethylation reaction using organotrifluoroborates. *J Org Chem* 2007;72:8422–8426. [PubMed: 17915931]
19. Luu KN, Phan AT, Kuryavvi V, Lacroix L, Patel DJ. Structure of the human telomere in K^+ solution: An intramolecular (3 + 1) G-quadruplex scaffold. *J Am Chem Soc* 2006;128:9963–9970. [PubMed: 16866556]
20. (a) Crothers DM. Statistical thermodynamics of nucleic acid melting transitions with coupled binding equilibria. *Biopolymers* 1971;10:2147–2160. [PubMed: 5118648] (b) McGhee JD. Theoretical calculations of the helix-coil transition of DNA in the presence of large, cooperatively binding ligands. *Biopolymers* 1976;15:1345–1375. [PubMed: 949539]
21. Tauchi T, Shin-ya K, Sashida G, Sumi M, Okabe S, Ohyashiki JH, Ohyashiki K. Telomerase inhibition with a novel G-quadruplex-interactive agent, telomestatin: *in vitro* and *in vivo* studies in acute leukemia. *Oncogene* 2006;25:5719–5725. [PubMed: 16652154]
22. Plum, GE. Optical methods. In: Beaucage, SL.; Bergstrom, DE.; Glick, GD.; Jones, RA., editors. *Current Protocols in Nucleic Acid Chemistry*. Vol. 1. John Wiley & Sons; New York: 2000. p. 7.3.1-7.3.17.
23. Andoh T, Ishii K, Suzuki Y, Ikegami Y, Kusunoki Y, Takemoto Y, Okada K. Characterization of a mammalian mutant with a camptothecin-resistant DNA topoisomerase I. *Proc Natl Acad Sci USA* 1987;84:5565–5569. [PubMed: 3039492]
24. Gervasoni JE Jr, Fields SZ, Krishna S, Baker MA, Rosado M, Thuraiamy K, Hindenburg AA, Taub RN. Subcellular distribution of daunorubicin in p-glycoprotein-positive and negative drug-resistant cell lines using laser-assisted confocal microscopy. *Cancer Res* 1991;51:4955–4963. [PubMed: 1680024]

25. Li TK, Houghton PJ, Desai SD, Daroui P, Liu AA, Hars ES, Ruchelman AL, LaVoie EJ, Liu LF. Characterization of ARC-111 as a novel topoisomerase I-targeting anticancer drug. *Cancer Res* 2003;63:8400–8407. [PubMed: 14679002]

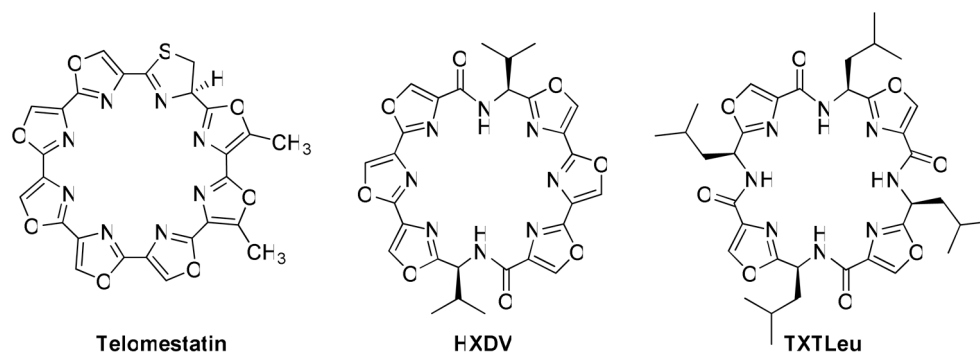


Figure 1.
Structures of telomestatin, HXDV, and TXTLeu.

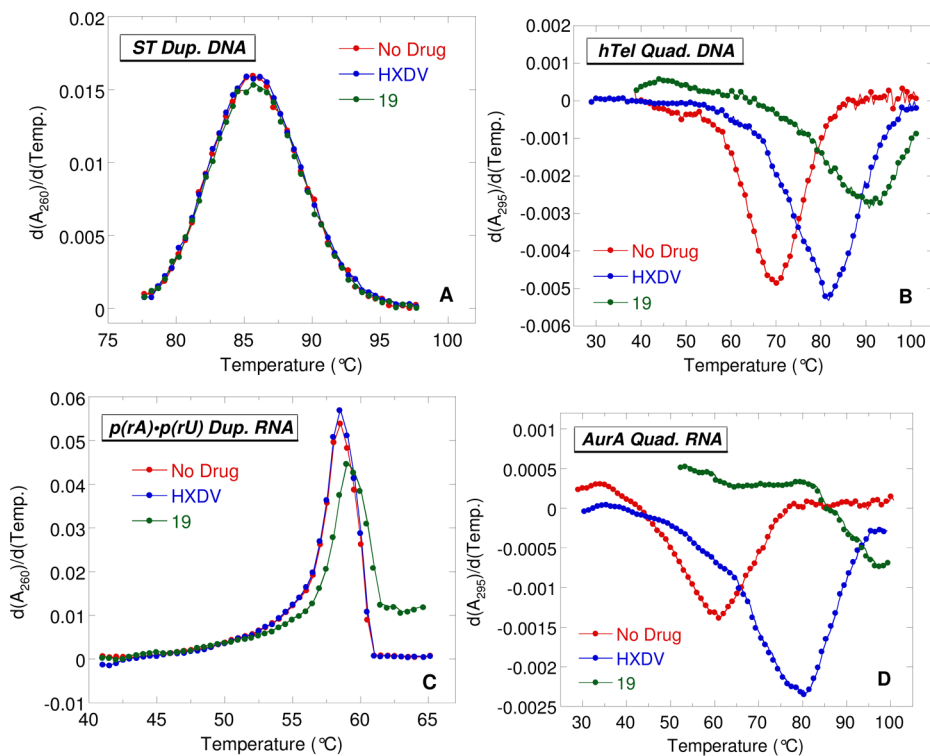


Figure 2.

First derivatives of the UV melting profiles of ST duplex DNA (**A**), hTel quadruplex DNA (**B**), poly(rA)•poly(rU) duplex RNA (**C**), and AurA quadruplex RNA (**D**) in the absence (red) and presence of either HXDV (blue) or **19** (green). The UV melting profiles of the quadruplexes were acquired at 295 nm, while those of the duplexes were acquired at 260 nm. In all experiments, the solution conditions were 10 mM potassium phosphate (pH 7.5) and sufficient KCl (132 mM) to bring the total K^+ concentration to 150 mM.

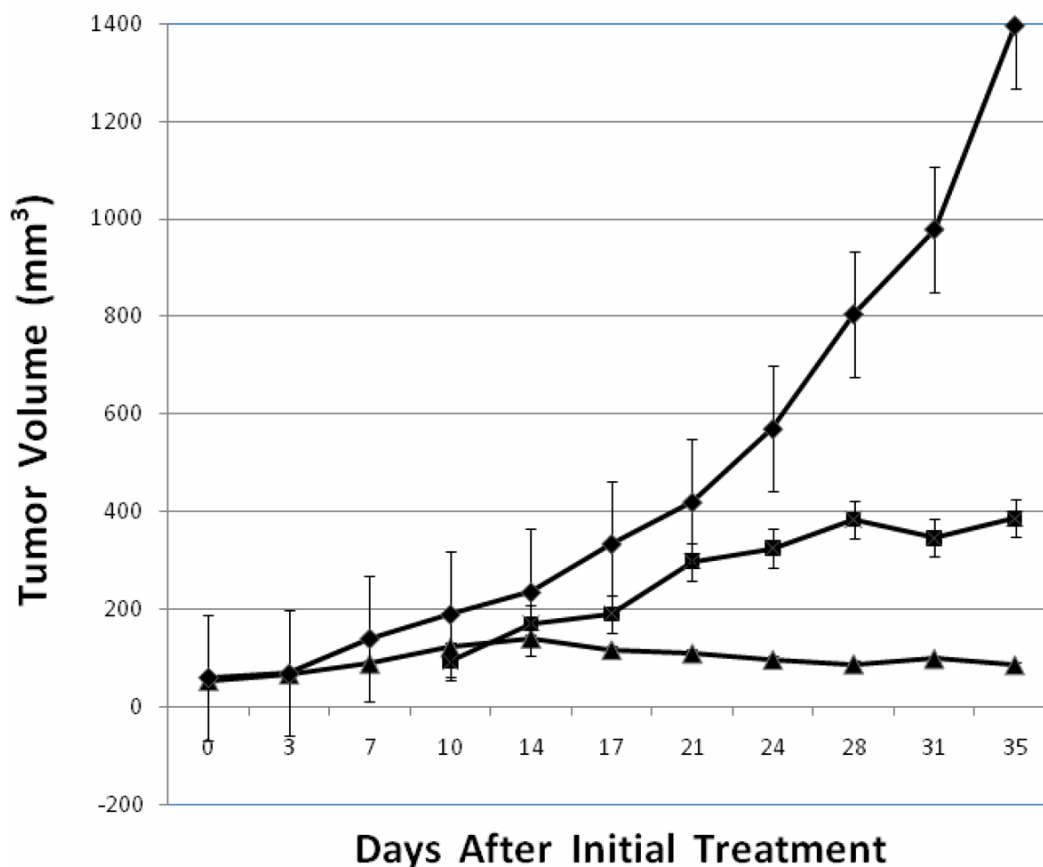
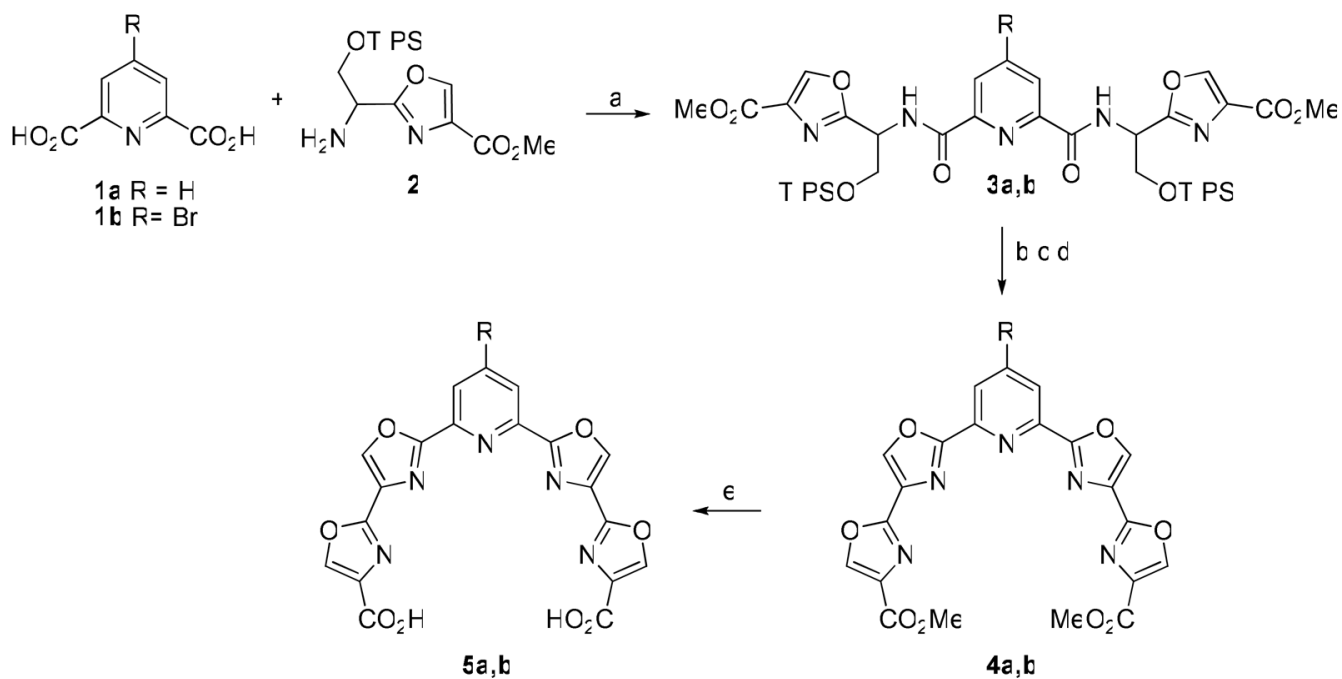
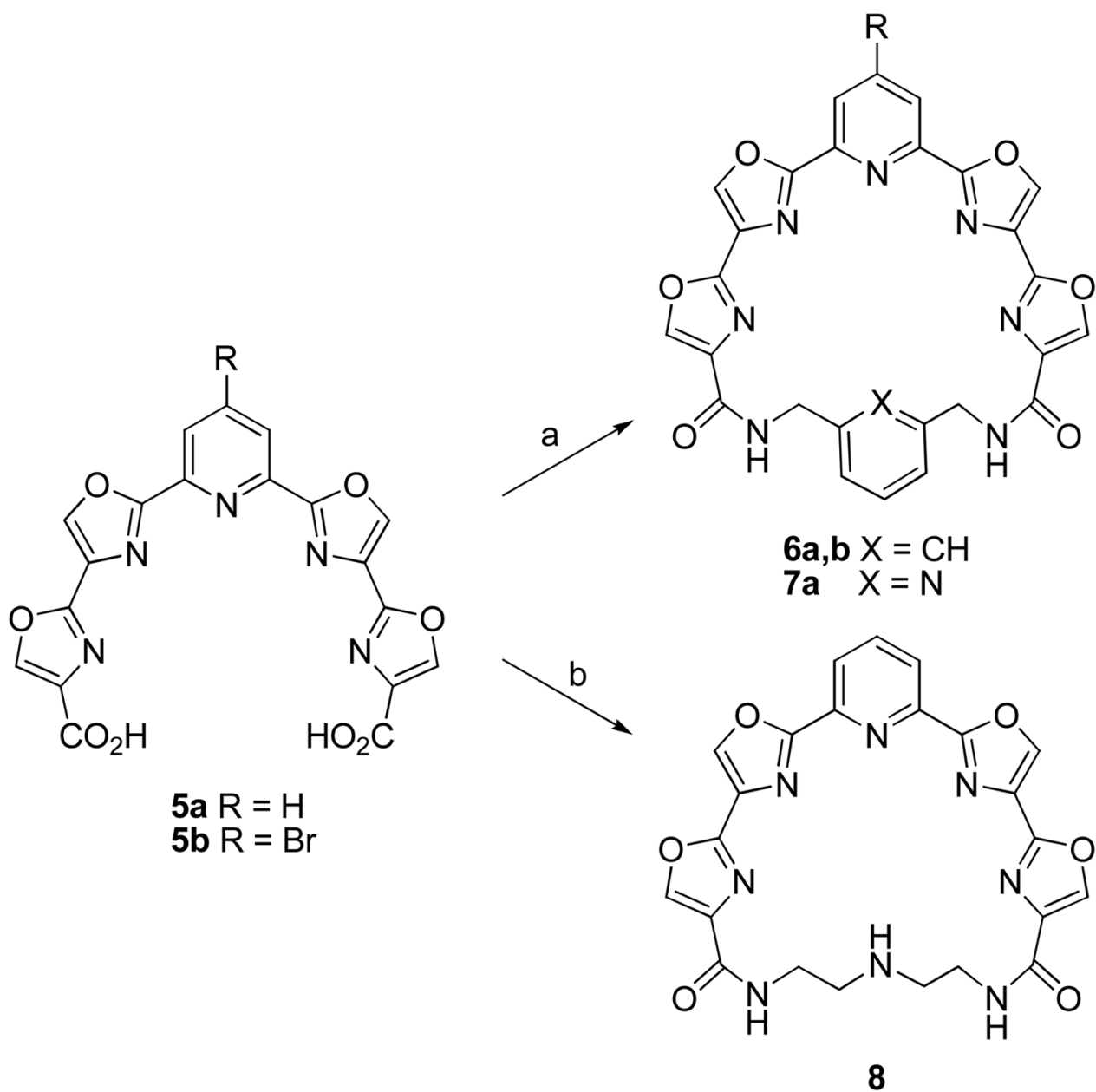


Figure 3.

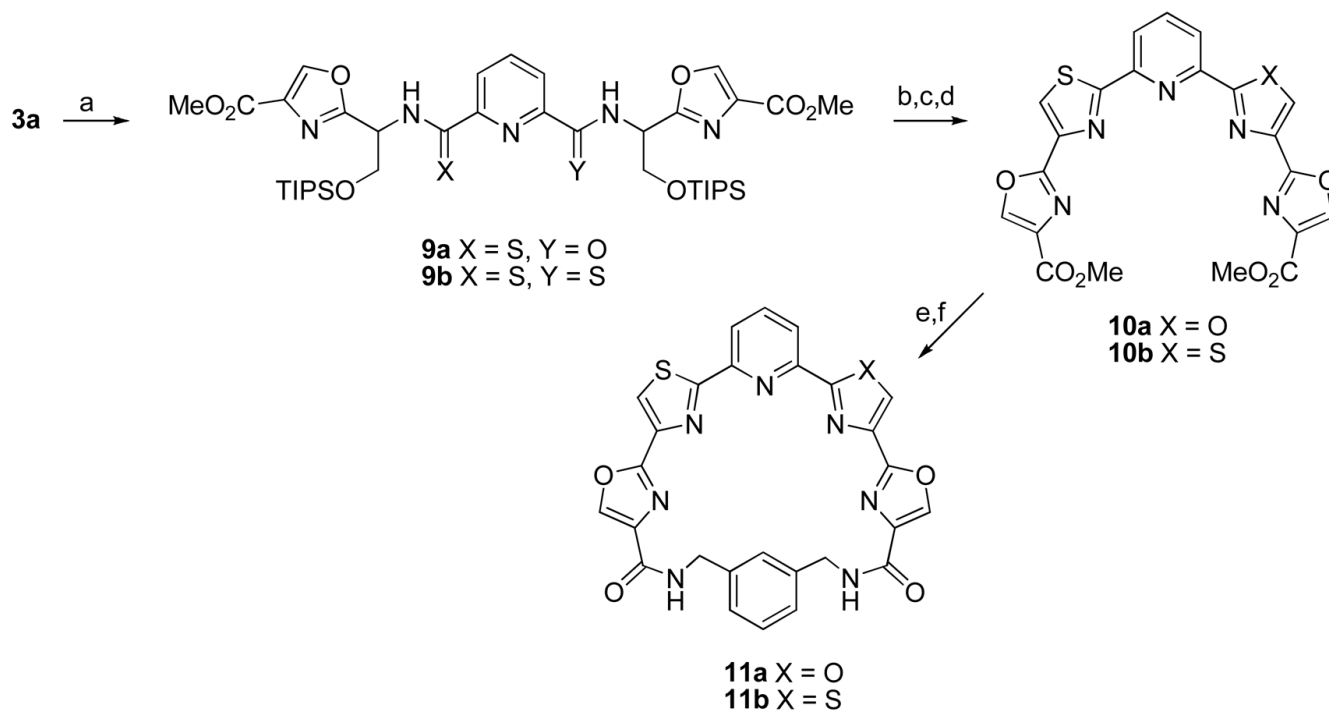
The test compounds, irinotecan (▲), 10 mM citrate (◆), and **19** (■) were administered by i.p. injection to athymic nude mice with human tumor xenografts established using MDA-MB-435 breast cancer cells. Mice were injected ip 3 × weekly. Negative controls (7 mice) were injected with 150 μl of 10 mM citrate. The positive control group (8 mice) received irinotecan by ip injection at a dose of 20 mg/kg, 3 × weekly, for all four weeks. Compound **19** was similarly administered to seven mice, 3 × weekly, at a dose of 25 mg/kg starting at week 2 with increasing doses of 32 and 42 mg/kg on weeks 3 and 4, respectively. Data are presented as the mean ± SE. The % T/C (average tumor volume of treated as compared to control group) is 27.7% for **19** and 6.1% for irinotecan.

**Scheme 1a.**

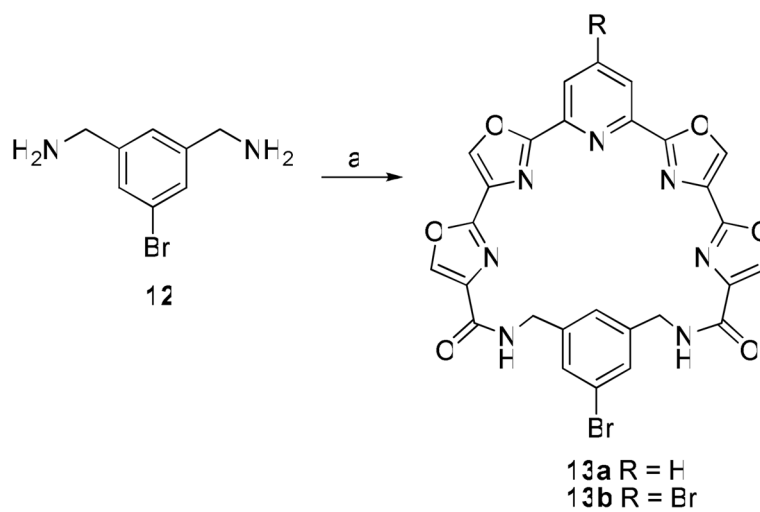
^a *Reagents and conditions:* (a) EDC, HOBT, 2,6-lutidine, DMF, 0 °C to rt; (b) HF-pyridine, rt; (c) DAST, CH₂Cl₂, -78 °C; (d) BrCCl₃, DBU, CH₃CN, 0 °C to rt; (e) for R=H, LiOH, THF/H₂O, Δ; for R=Br, LiBr, DBU, THF/H₂O, Δ.

**Scheme 2a.**

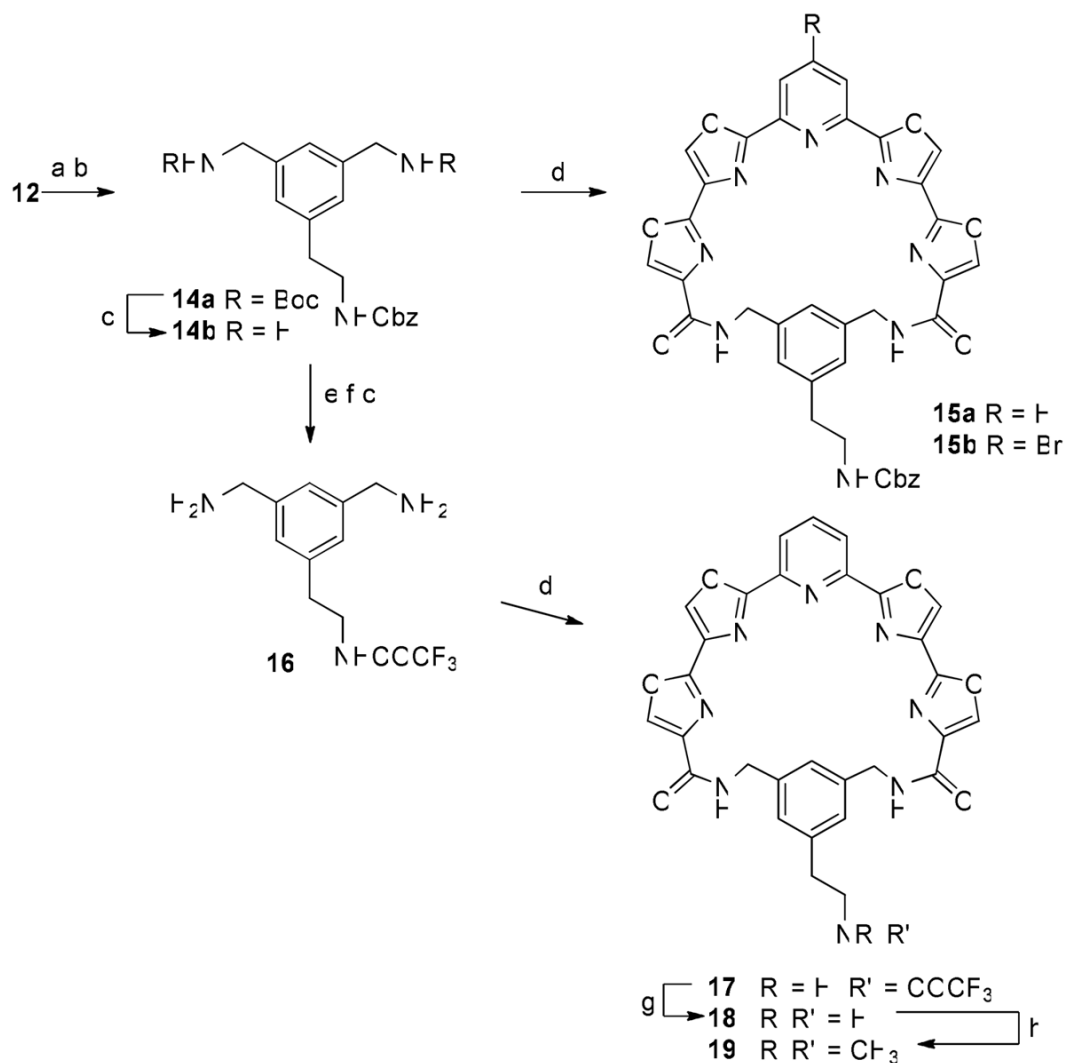
^a *Reagents and conditions:* (a) **5a** or **5b** (2 mM in DMF), EDC, HOBT, 2,6-lutidine, 1,3-bis(aminomethyl)benzene or 2,6-bis(aminomethyl)pyridine, rt, 2 d; (b) **5a** (0.53 mM in DMF), Cu(OTf)₂, 2 h, rt then EDC, HOBT, 2,6-lutidine, diethylenetriamine, rt, 2 d.

**Scheme 3a.**

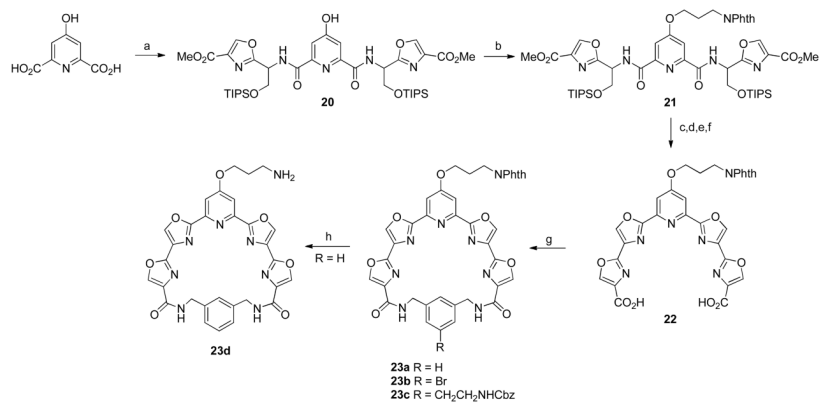
^a *Reagents and conditions:* (a) Lawesson's reagent (1 equiv for **9a**, excess for **9b**), toluene, 80 °C; (b) HF-pyridine, rt; (c) DAST, CH₂Cl₂, -78 °C; (d) BrCCl₃, DBU, CH₂Cl₂, 0 °C to rt; (e) LiOH, THF/H₂O, Δ; (f) (2 mM in DMF), EDC, HOBT, 2,6-lutidine, 1,3-bis(aminomethyl) benzene rt, 2 d.

**Scheme 4a.**

^a Reagents and conditions: (a) **5a** or **5b** (2 mM in DMF), EDC, HOBT, 2,6-lutidine, rt, 2 d.

**Scheme 5a.**

^a Reagents and conditions: (a) Boc_2O , Et_3N , CH_2Cl_2 , rt; (b) $\text{CbzNHCH}_2\text{CH}_2\text{BF}_3\text{K}$, $\text{PdCl}_2(\text{dppf}) \cdot \text{CH}_2\text{Cl}_2$, Cs_2CO_3 , toluene/ H_2O , 80°C ; (c) TFA , CH_2Cl_2 , 0°C ; (d) **5a** or **5b** (2 mM in DMF), EDC , HOBT , 2,6-lutidine, rt, 2 d; (e) 1 atm H_2 , 20% $\text{Pd}(\text{OH})_2/\text{C}$, EtOH , rt; (f) TFAA , pyridine, CH_2Cl_2 , 0°C ; (g) K_2CO_3 , MeOH , Δ ; (h) HCHO (aq), $\text{NaBH}(\text{OAc})_3$, $\text{MeOH}/\text{CH}_2\text{Cl}_2$, rt.

**Scheme 6a.**

^a Reagents and conditions: (a) **2**, EDC, HOBT, 2,6-lutidine, DMF, 0 °C to rt; (b) Br(CH₂)₃NPhth, DBU, DMF, 60 °C; (c) HF-pyridine, rt; (d) DAST, CH₂Cl₂, -78 °C; (e) BrCCl₃, DBU, CH₂Cl₂, 0 °C to rt; (f) LiCl, DMF, Δ; (g) 1,3-bis(aminomethyl)benzene or **12** or **14**, (2 mM in DMF), EDC, HOBT, 2,6-lutidine, rt, 2 d; (h) H₂NNH₂·H₂O, EtOH, Δ.

Table 1Cytotoxicity of macrocyclic pyridyl polyoxazoles^a

Compound	IC ₅₀ (μM)			
	RPMI 8402	KB3-1 wt	KBV-1 + MDR1	KBH5.0 + BCRP
HXDV	0.6	0.4	8.5	0.5
6a	1.05	1.2	4.5	1.5
6b	0.3	0.15	2.0	1.0
7a	>5	>5	>5	>5
8	>10	4.0	>10	>10
11a	1.0	0.26	>10	>10
11b	>10	>10	>10	>10
13a	0.3	0.06	>10	1.0
13b	>10	>10	>10	>10
15a	0.12	0.12	>10	>10
15b	1.0	0.6	>10	>10
17	0.17	0.07 ^b	>10 ^b	>10 ^b
18	0.09	0.03 ^b	>10 ^b	0.14 ^b
19	0.18	0.04 ^b	>10 ^b	0.55 ^b
23a	4.5	0.4	>10	>10
23b	1.0	1.0	>10	>10
23c	>10	>10	>10	>10
23d	5.0	3.0	>10	>10

^aValues represent the average of three experiments.^bValues represent the average of four experiments.

Table 2

Impact of HXDV and Various Macrocyclic Pyridyl Polyoxazoles on the Thermal Stabilities of the Duplex and Quadruplex Forms of DNA and RNA

Compound	Change in Thermal Stability, ΔT_{tran}^a (°C)			
	ST Duplex DNA	poly(rA)•poly(rU) Duplex RNA	hTel Quadruplex DNA	AurA Quadruplex RNA
HXDV	0	0	11.5	19.5
6a	0	0	7.5	ND
11b	0	0	0	ND
18	0	0.5	21.0	ND
19	0	0.5	20.5	37.0

^a ΔT_{tran} reflects the change in transition temperature (T_{tran}) of the target nucleic acid induced by the presence of the compound. Values of T_{tran} were determined from the maxima or minima of first-derivative UV melting profiles exemplified by those shown in Figure 2. The uncertainty in the ΔT_{tran} values is ± 0.5 °C. ND denotes not determined.

Table 3Average body weights of athymic nude mice treated with citrate, **19**, and irinotecan.

<u>Average body weight \pm standard deviation (g)</u>			
Day	Citrate	Compd 19	Irinotecan
17	22.0 \pm 1.8	19.7 \pm 1.9	19.5 \pm 1.3
24	22.5 \pm 1.5	20.2 \pm 2.3	19.8 \pm 1.4
31	23.9 \pm 1.0	20.9 \pm 2.4	18.4 \pm 2.0 ^a
35	24.6 \pm 1.3 ^b	21.1 \pm 1.9	20.7 \pm 1.6

^a One cage of four mice was found not to have a water bottle, which is reflected the drop in average weight on day 31.

^b One mouse was euthanized on day 31 because the tumor volume was 2,266 mm³, which exceeded protocol limitations.